

Feature Article

Polymer memories: Bistable electrical switching and device performance

Qi-Dan Ling ^a, Der-Jang Liaw ^b, Eric Yeow-Hwee Teo ^c, Chunxiang Zhu ^c, Daniel Siu-Hung Chan ^c,
En-Tang Kang ^{a,*}, Koon-Gee Neoh ^a

^a Department of Chemical and Biomolecular Engineering, National University of Singapore, 10 Kent Ridge Crescent, Singapore 119260, Singapore

^b Department of Chemical Engineering, National Taiwan University of Science and Technology, 43, Section 4, Keelung Road, Taipei, Taiwan

^c SNDL, Department of Electrical and Computer Engineering, National University of Singapore, 10 Kent Ridge Crescent, Singapore 119260, Singapore

Received 29 April 2007; received in revised form 9 June 2007; accepted 13 June 2007

Available online 21 June 2007

Abstract

As an emerging area in organic electronics, polymer memories have become an active research topic in recent years. Polymer memories based on bistable electrical switching are likely to be an alternative or supplementary technology to the conventional memory technology facing the problem in miniaturizing from micro- to nano-scale. In this article, an account of our recent work on bistable electrical switching in a series of processable electroactive polymers is given. The polymers can provide the required electronic properties within a single macromolecule for memory device applications. Bistable electrical switching phenomena arising from four processes, *viz.*, trapping–detrapping, charge transfer, conformational change and nanocomposite redox effects, in electroactive polymers are described. In each case, three aspects of the memory effect, *viz.*, (i) materials and structural features, (ii) conductance switching and current–voltage characteristics, and (iii) operating mechanism and electronic transitions are emphasized. Finally, the performance of these polymer memories is summarized.

© 2007 Elsevier Ltd. Open access under [CC BY-NC-ND license](http://creativecommons.org/licenses/by-nc-nd/2.0/).

Keywords: Polymer; Electronics; Bistable switching

1. Introduction

The amazing success of microelectronics over the past 40 years is based to a large extent on advances in the fabrication of silicon-based integrated circuits. However, a number of physical and economic factors, which threaten the continued scaling down of silicon semiconductor devices, have motivated research into electronic systems based on other technologies [1–3]. Organic materials are promising candidates for future molecular-scale device applications. Their attractive features include miniaturized dimensions and the possibility for molecular design through chemical synthesis [4,5]. It has been demonstrated that individual or small packets of molecules, mounted within addressable scaffolds, can conduct and switch electrical currents, and can retain electrical bits

of information [6]. A wide variety of organic materials, including organic dyes [7–10], charge transfer (CT) complexes [11–15], conjugated oligomers [16–18], redox metal complexes [19–21] and other molecules [22–25], have been explored for memory applications. Rather than encoding “0” and “1” as the amount of charge stored in a cell in silicon devices, organic memory stores data in an entirely different form, for instance, based on the high- and low-conductivity response to an applied voltage [26]. Advantages of polymer and organic memories include simplicity in device structure, good scalability, low-cost potential, low-power operation, multiple-state accessibility, three-dimensional (3D) stacking capability and large capacity for data storage [27–34]. In particular, polymer materials possess unique properties, such as good mechanical strength, flexibility, and most important of all, ease of processing [35,36]. As alternatives to the more elaborated processes of vacuum evaporation and deposition of inorganic and organic molecular materials, other solution processes, including spin-coating, spray-coating, dip-coating, roller-coating and

* Corresponding author. Tel.: +65 6516 2189; fax: +65 6779 1936.

E-mail address: cheket@nus.edu.sg (E.-T. Kang).

ink-jet printing, are well known in the art and can be used to deposit polymers on a variety of substrates (plastics, wafers, glass and metal foils) [34].

A number of polymeric materials, including a composite material of poly(ethylenedioxythiophene) and poly(styrene-sulfonic acid) (or PEDOT:PSS) [37], a mixture of gold nanoparticles, 8-hydroxyquinoline and polystyrene [38], supra-molecular structures doped with dyes [7], and other polymer CT complexes [39] have been explored for polymer memory effects and applications. Most of the polymers in these pioneering works were used as the polyelectrolyte, matrix of a dye, or component of a CT complex in a doped or mixed system. Doping or mixing of incompatible components may give rise to non-uniform dispersion, resulting in phase separation and ion aggregation [40].

We have embarked on the design and synthesis of a series of processable polymers, which can provide the required electronic properties within a single macromolecule and yet still possess good chemical, mechanical and morphological characteristics, for memory device applications. The molecular design-cum-synthesis approach has allowed several polymer memories, including flash (rewritable) memory, WORM (write-once read-many-times) memory and dynamic random access memory (DRAM) to be realized. In this feature article, we summarize our recent work on these polymer memories. A more comprehensive review on the topic of molecular and polymer memories will appear in the second edition of Encyclopedia of Nanoscience and Nanotechnology [26].

2. Device structure and fabrication method

The memory cell test structure consists of an electroactive polymer thin film sandwiched between two electrodes on a supporting substrate (plastics, wafer, glass or metal foil), as shown in Fig. 1(a). The configuration of electrodes can be symmetric or asymmetric, with Al, Au, Cu, p- or n-doped Si, and indium-tin oxide (ITO) as the most widely used electrode materials. The basic memory cells can be integrated into a cross point memory array. A schematic diagram of a 4 (word

line) \times 4 (bit line) crossbar memory device is shown in Fig. 1(b). Each memory cell is univocally identified by its *X* and *Y* coordinates and this kind of selection is used both for programming and for reading the desired cell. Cross point memory arrays are two terminal devices. The arrays can be stacked to form three-dimensional (3D) data storage devices. A schematic diagram of a 2 (stacked layer) \times 4 (word line) \times 4 (bit line) stacked memory device is shown in Fig. 1(c). Inside each memory layer, cells are arranged in two-dimensional arrays. Stacked multilayer memories offer high data storage density and simplicity in device fabrication, to overcome the limitations of conventional lithographic process.

Polymer memory fabrication is a bottom-up approach. By contrast, silicon memory fabrication is a top-down approach, involving etching away of a silicon crystal to form micrometer-sized devices and circuitry. Bottom-up approach gives rise to the prospect of manufacturing electronic circuits in rapid and cost-effective flow-through processes. In the typical fabrication of test structures, a polymer solution is spin-coated onto the bottom electrode (such as ITO) to provide a polymer film of ~ 50 nm thickness. Complete solvent removal is achieved by heating in a vacuum chamber. The top electrodes of 0.4×0.4 , 0.2×0.2 and 0.15×0.15 mm² area, and several hundred nanometers in thickness, are thermally evaporated onto the polymer surface at a reduced pressure of about 10^{-5} Pa through a shadow mask. The devices are characterized, under ambient conditions, using a Hewlett-Packard 4156A semiconductor parameter analyzer equipped with an Agilent 16440A SMU/pulse generator.

3. Bistable electrical switching based on trapping–detrapping processes in polymers

3.1. Materials and structural features

Certain electroactive polymers containing electron donor and electron acceptor moieties exhibit bistable electrical switching behavior arising from carrier trapping–detrapping processes. Three representative classes of polymer materials

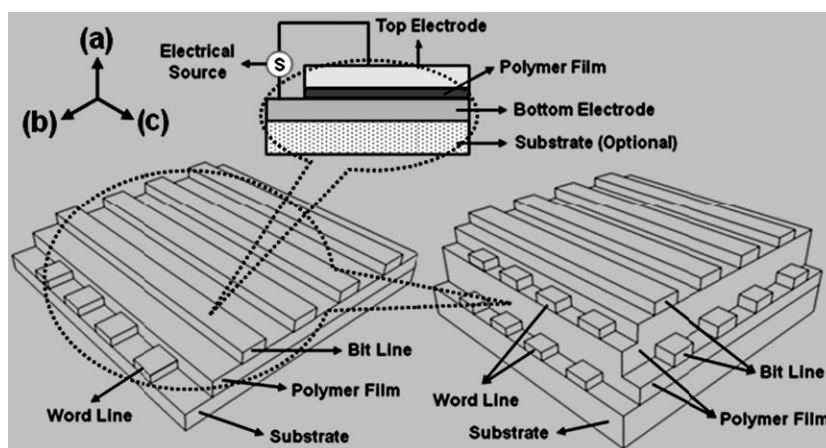


Fig. 1. (a) The basic configuration of a polymer memory cell. (b) Schematic diagram of a 4 (word line) \times 4 (bit line) cross point memory array. (c) Schematic diagram of a 2 (stacked layer) \times 4 (word line) \times 4 (bit line) stacked memory device.

for the trapping–detrapping memories are shown in Scheme 1. PKEu and PCzOxEu are non-conjugated polymers containing carbazole group as the electron donor (D) and europium complex as the electron acceptor (A). PF6Eu and PF8Eu are conjugated polymers containing the fluorene group as the electron donor and europium complex as the electron acceptor. PFOxPy is a conjugated polymer containing the fluorene group as the electron donor, and the oxadiazole and bipyridine groups as the electron acceptors.

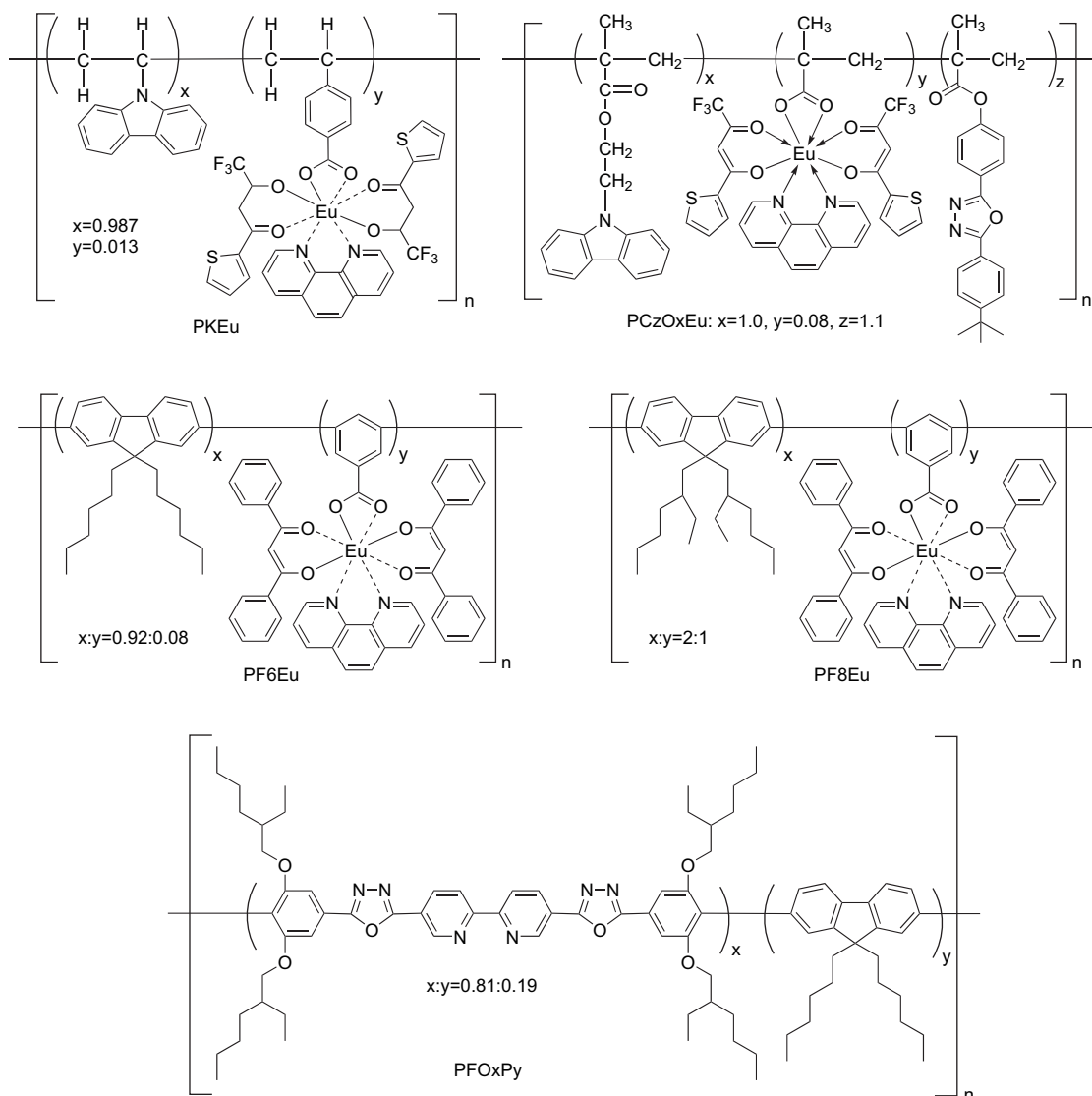
3.2. Memory effects and current–voltage characteristics

The memory effects of devices based on different materials are summarized in Table 1. The devices based on PKEu and PCzOxEu exhibit the ability to write, read, erase and retain the stored state. They are non-volatile and rewritable flash memories. The devices based on PF6Eu and PF8Eu exhibit the ability to write and read. The ON-state cannot be erased but is retained permanently. Thus, they are write-once read-

many times (WORM) memories. The device based on PFOxPy exhibits the ability to write, read and erase. The retention time of the ON-state is very short, but the ON-state can be electrically sustained by a refreshing voltage pulse every few seconds. These abilities fulfil the functionality of a dynamic random access memory (DRAM).

3.2.1. Flash memory effect from non-conjugated polymers containing metal complex

Flash memory is a type of non-volatile memory, which does not require power to retain the information stored in the cell. It can be electrically erased and reprogrammed. Flash memories are widely used in portable systems, such as PDA, mobile PC, video/audio player and digital camera. Current flash memory technology is based on metal-oxide-semiconductor field-effect transistor (MOSFET) with a floating gate. Electric field can transfer charge to and from the floating gate and modifies the threshold voltage (encoding “0” and “1” signals) of the underlying transistor. Flash memory effect can also be realized



Scheme 1. Chemical structures of some polymer materials exhibiting trapping–detrapping-induced memory effects.

Table 1
Structural features and memory effects of different classes of polymer materials

Materials	Structural features				Memory effects						
	Conjugate	e-Donor	e-Acceptor	Complex	Write	Read	Erase	Retain	Refresh	Rewritable	Volatile
PKEu, PCzOxEu	×	✓	✓	✓	✓	✓	✓	✓	O	✓	×
PF6Eu, PF8Eu	✓	✓	✓	✓	✓	✓	×	✓	O	×	×
PFOxPy	✓	✓	✓	×	✓	✓	✓	×	+	✓	✓

✓ – Yes or able; × – not or unable; + – necessary; O – unnecessary.

in many polymer materials based on their resistance changes in response to an applied voltage [27].

In our copolymer system, the devices based on non-conjugated polymers containing electron D–A structure and metal complex exhibit flash memory effect [41,42]. Fig. 2 shows the typical current density–voltage (J – V) characteristics of the Al/PKEu/ITO sandwich device [41]. J increases progressively with the applied bias (stage I). A sharp decrease in current occurs at about 4 V (stage II), indicating the transition of the device from the high conductivity state (ON-state) to a low conductivity state (OFF-state). This transition from the ON-state to the OFF-state is equivalent to the “writing” process in a digital memory cell [41]. After this transition, the device remains in this state even after the power is turned off. This phenomenon can be seen in the third scan (stage III) in Fig. 2. The J – V characteristics define the electrical bistability of the PKEu and also reveal the non-volatile nature of the memory effect. The OFF-state can be recovered by the simple application of a reverse voltage pulse (at about -2 V, stage IV). This is equivalent to the “erasing” process of a digital memory cell. Stage V of Fig. 2 shows the J – V characteristics of the device after application of a -2 V bias. The behavior is nearly identical to that of stage I. This feature allows the application of PKEu in a rewritable flash memory [41]. Similar memory behavior has also been observed in a series of rare earth metal complexes, including Eu(DBM)₃(tmphen), Sm(DBM)₃(tmphen) and Gd(DBM)₃(bath), doped into poly(*N*-vinylcarbazole) (PVK) as active medium in the memory

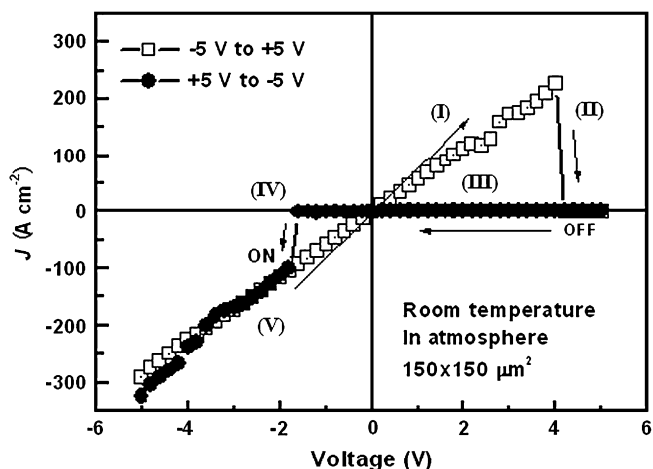


Fig. 2. Current density–voltage (J – V) characteristics of the Al/PKEu/ITO device based on a spin-cast film of PKEu (~ 50 nm) for two sweep directions. Arrows indicate the sweep direction of the applied voltage (Ref. [41]).

devices (DBM = dibenzoylmethane, tmphen = 3,4,7,8-tetra-methyl-1,10-phenanthroline, bath = 4,7-diphenyl-1,10-phenanthroline) [43].

3.2.2. WORM memory effect from conjugated polymers containing metal complex

WORM memory is a type of non-volatile memory that is capable of holding data permanently and being read from repeatedly. It can be written only once physically, and it is not feasible to modify the stored data. WORM memory can be used to store archival standards, databases and other massive data where information has to be reliably kept and made available over a long period of time. In these cases, WORM memory functions as the conventional CD-R, DVD \pm R or PROMs. WORM memory can also be used as disposable memory in some niche environments, such as electronic labels and RFIDs.

The devices based on conjugated polymers containing electron D–A structure and metal complex exhibit the WORM memory effect [41,44–48]. The memory effect of PF6Eu is shown in the J – V characteristics of the device Al/PF6Eu/ITO in Fig. 3. Initially, the as-fabricated device is at its low conductivity state (OFF-state). The current density in the low voltage range on the first sweep is quite low (of the orders of 10^{-10} – 10^{-8} A/cm²). When a switching threshold voltage of about 3 V is applied, an abrupt increase in J from 10^{-8} to 10^{-2} A/cm² is observed, indicating the device transition

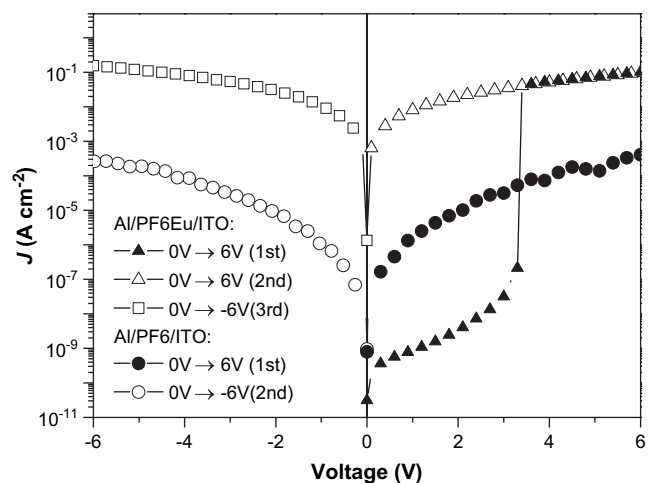


Fig. 3. Typical J – V characteristics of the Al/PF6Eu/ITO device in the ON- and OFF-state and the J – V curves of the Al/PF6/ITO device based on conjugated poly(9,9-dihexylfluorene) (PF6) without the europium complex moiety (Ref. [44]).

from a low conductivity state to a high conductivity state (ON-state, the first sweep) [44]. This electrical transition from the OFF-state to the ON-state serves as the “writing” process for the memory device. The device exhibits good stability in this high conductivity state during the subsequent forward and reverse voltage scans (Fig. 3). It remains in the ON-state even after turning off the power (the second sweep) and does not return to the low conductivity state upon applying a negative bias (the third sweep). Thus, this device exhibits the WORM-type memory effect [44]. For the same class of conjugated copolymers containing europium complex with different substituted alkyl group [45], composition [46] or coordination ligands [48], the devices exhibit similar WORM memory effect. When n-type silicon substrate is used as the bottom electrode instead of ITO (Al/PF6Eu/n-Si), diode rectifying characteristics were observed for the turned-on device with a current ratio of 7×10^4 . This feature is essential to address one memory cell in large passive matrix circuits [47]. Without the rectifying characteristics, parasitic paths may exist in parallel to the selected node, through all the neighboring nodes [49]. These paths can affect the reading process, introducing parasitic leakage currents, and hinder programming in passive array or cross point memories [50]. A flexible WORM memory device based on P6FBEu has been demonstrated with a conductive polypyrrole film as the bottom electrode and gold as the top electrode [48]. The flexible polymer memory is expected to meet the demand for data storage in memory devices of unique spatial construct or architecture, such as smart label and RFID.

3.2.3. DRAM effect from conjugated polymers without metal complex

DRAM is a random access memory that stores each bit of data in a separate capacitor. As the real-world capacitors have tendency to leak electrons, the information eventually fades unless the capacitor charge is refreshed periodically. Because of this refresh requirement, it is a dynamic memory. Since DRAM loses its data when the power supply is removed, it is in the class of volatile memory devices. Currently, DRAM is used as the main memory of most computers.

To realize the DRAM effect, a special polymer, PFOxPy, has been designed and synthesized [51]. It is a conjugated polymer containing the fluorene group as the electron donor, and the oxadiazole and bipyridine groups as the electron acceptors. The J - V characteristics of the device based on PFOxPy is shown in Fig. 4. The device, ITO/PFOxPy/Al, is swept negatively with the sweep direction indicated by the arrows. Initially, the device is at its low conductivity state (OFF-state). The current density in this state is quite low (of the orders of 10^{-9} – 10^{-7} A/cm²). When a switching threshold voltage of about -2.8 V (onset) is applied, an abrupt increase in J from 10^{-7} to 10^{-2} A/cm² is observed, indicating the device transition from a low conductivity state to a high conductivity state (ON-state). This electrical transition serves as the “writing” process for the memory device [51]. Subsequent forward and backward sweeps show that the device remains in its high conductivity state. The distinct bi-electrical states in the

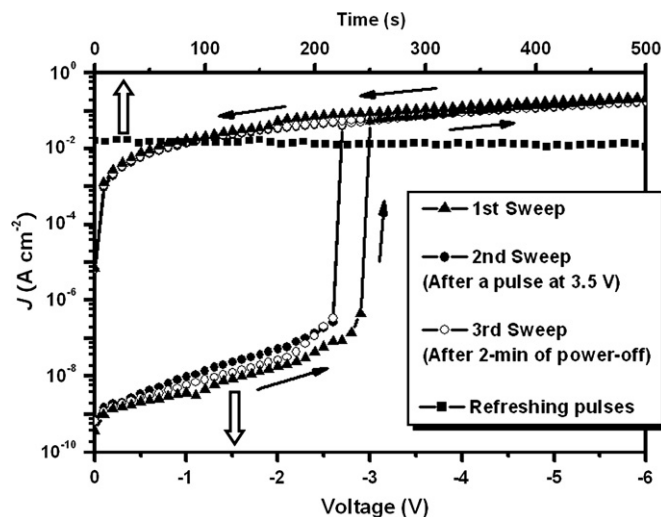


Fig. 4. J - V characteristics of the ITO/PFOxPy/Al device in the ON- and OFF-state, and maintaining the ON-state by refreshing at -1 V every 10 s (Ref. [51]).

voltage range of about 0 V to -2 V allow the use of a voltage (e.g., -1.0 V) to read the “0” or “OFF” signal (before writing) and “1” or “ON” signal (after writing) of the memory. As indicated in the 2nd sweep after a reverse voltage pulse of about 3.5 V, the memory device can be reset to the initial low conductivity state (“0” or OFF-state), corresponding to the “erasing” process for the memory device. The erased state (“0”) can be further written to the stored state (“1”) when the switching threshold voltage is applied, indicating that the memory device is rewritable. The slightly higher turn-on voltage for the 1st sweep might have been caused by the initial delay in conformational change of the polymer chain under the electric field. The 3rd sweep is carried out after turning off the power for about 2 min. It is found that the ON-state has relaxed to the steady OFF-state [51]. However, the device can be further programmed to the ON-state. The short retention time of the ON-state indicates that the memory device is volatile. However, the ON-state can be electrically sustained by a refreshing voltage pulse of -1 V in every 10 s (Fig. 4, solid square curve). The above characteristics are repeatable with high accuracy and device degradation is not observed. This ability to write, read, erase and refresh the electric states of the device fulfils the functionality of a DRAM [51].

3.3. Operating mechanism and electronic processes

The flash, WORM and DRAM memory effects of these polymers can be explained by electronic processes of carrier trapping–detrapping. Fig. 5(a) and (b) shows the highest occupied molecular orbitals (HOMO), the lowest unoccupied molecular orbitals (LUMO) and their energy levels for the PFOxPy segments calculated from the density function theory (DFT). The work functions (Φ) of ITO and Al electrodes are also shown in Fig. 5(a). The energy barrier between the Φ of ITO and the HOMO level is very low (0.4 eV), indicating that hole injection from ITO into the HOMO of PFOxPy is

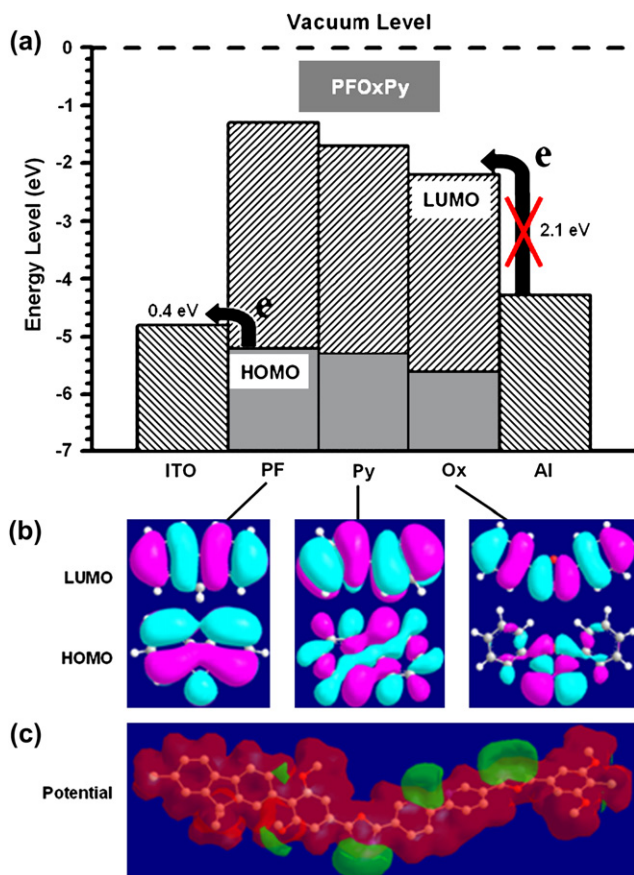


Fig. 5. (a) and (b) show the HOMO, LUMO energy levels and orbitals for the PFOxPy segments calculated from the density function theory (DFT). (c) Molecular electrostatic potential (ESP) surfaces of the basic unit of PFOxPy (hydrogen atoms are hidden for a clear view) (Ref. [51]).

the favored process. On the contrary, electron injection from Al into the LUMO of PFOxPy is much more difficult due to the high barrier between the LUMO and the Φ of Al (2.1 eV). Thus, PFOxPy is a p-type material and holes will originally dominate the conduction process. Fig. 5(c) shows a molecular surface with continuous positive electrostatic potentials (ESP) (in red color) along the conjugated backbone, indicating that charge carriers can migrate through this open channel. However, there are some negative electrostatic potential regions (in green color) lateral to the conjugated backbone. These negative regions arise from the electron acceptor groups and can serve as traps to block the mobility of charge carriers.

The electronic processes and experimental J - V curve fitting are shown in Fig. 6(a), (b) and (c), respectively. Under a low bias voltage (0 V to -1.3 V), the J - V curve is linear and can be fitted with the Ohmic model. The material is insulating with a resistance of about $10^9 \Omega$, and the device is at its OFF-state. When the voltage exceeds the Schottky barrier (-1.3 V), holes are injected from the ITO into the polymer. The existence of traps in polymer can lead to an accumulation of space charges and a redistribution of the electric field. Thus, the Ohmic current changes to the space charge limited current. At the turn-on voltage (-2.8 V), the generated carriers fill some of the charge traps and the Al cathode also becomes

an electron-injecting contact, leading to double injections. Under such condition, most traps become filled, leading to enhanced carrier concentration and mobility. The current increases rapidly to switch the sample to the high conductivity state (ON-state). At the ON-state, the J - V curve again follows the Ohmic model, with a room-temperature resistance in the order of $10^3 \Omega$.

In the case of PFOxPy, the charge traps of oxadiazole groups are shallow (0.6 eV), thus, the filled traps can be easily detrapped and the device behaves as a DRAM. In the case of conjugated polymers containing metal complexes, the charge traps are much deeper. For example, the trap depth of the europium complex in PF6Eu is 2.0 eV. Thus, it is difficult to detrapp (or detrapping will require a voltage higher than the break-down voltage of the device), and the device behaves as a WORM memory. PF6Eu is a p-type material with the holes as the dominant charge carriers. As a conjugated polymer, delocalized charge carriers can migrate through the π -conjugated backbone of the fluorene group. The current density of the device based on PF6Eu is much lower than that based on the Eu-free poly(9,9-dihexylfluorene) (PF6) in the low voltage range during the first sweep (Fig. 3) [44]. Eu complex is an electron-deficient complex and can act as an electron acceptor to block the charge carriers (holes) [52]. The europium complexes along the conjugated backbone in the copolymer probably serve as 'temporary barriers' to block the charge carriers. Thus, there are not many free charge carriers in PF6Eu and the presence of both the long alkyl side chains in fluorene and the bulky Eu complex substituent in the present copolymer reduces interchain interactions and interchain carrier hopping. Thus, the device is at its low conductivity state in the low voltage range during the first sweep. With the increase in applied voltage, the electric field exceeds the energy barriers for Al/fluorene (HOMO -5.66 eV) contact (1.38 eV) and the ITO/Eu complex (LUMO -3.50 eV) contact (1.34 eV) [44], electrons are injected into the LUMO of the Eu complexes and holes are injected into the HOMO of the fluorene moieties. The charged LUMO (radical anion) of the Eu complex and the charged HOMO (radical cation) of the fluorene moiety form a channel for charge carriers through non-radiative intersystem transition. The polymer becomes p-doped under the induction of the electric field and switches to the high conductivity state (ON-state). Due to the high electron affinity (EA) of the Eu complex (4.0 eV), as determined from cyclic voltammetry (CyV) results, the radical anions can coexist with the surrounding radical cations of the fluorene moieties. The 'doped state' of PF6Eu is stable and the high conductivity state can be maintained. Thus, the devices based on PF6Eu and its analogues exhibit WORM memory effect.

For the case of non-conjugated polymers containing carbazole group as the electron donor and europium complex as the electron acceptor, the europium complex can further form an insulating charge transfer (CT) complex with the carbazole group under an electric field. Charge carriers are trapped in the insulating CT complex. However, the CT complex can decompose under reverse bias. Thus it is a rewritable and non-volatile memory or flash memory [41,42]. Fig. 7 depicts the

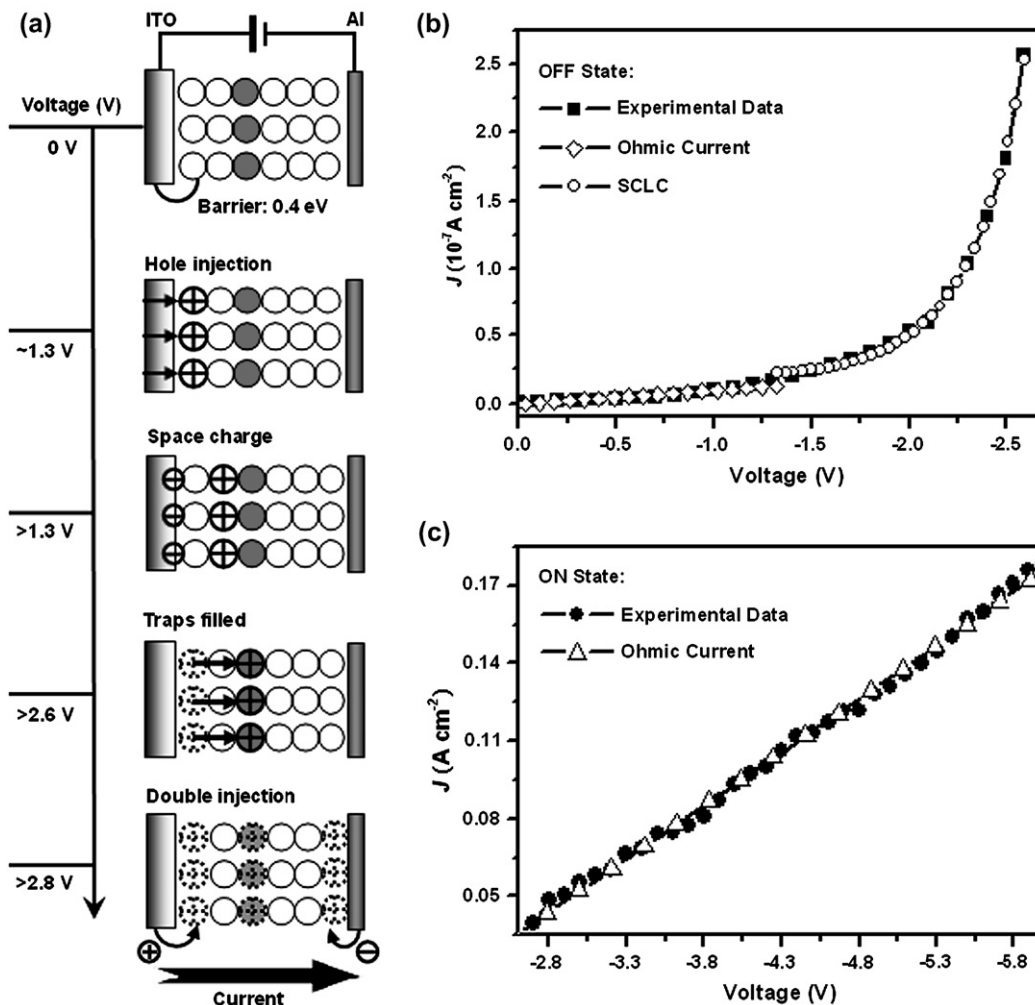


Fig. 6. (a) Operating mechanism of the memory. Experimental and fitted J - V curves of the ITO/PFOxPy/Al device. (b) OFF-state with the Ohmic current (<1.3 V) and space charge limited current (SCLC, ~ 1.3 – 2.6 V) models. (c) ON-state with the Ohmic current model (>2.8 V) (Ref. [51]).

operating mechanism and electronic processes of the device Al/PKEu/ITO. The high conductivity state (ON) of PKEu is similar to that of PVK since the carbazole groups are the dominant moieties in the copolymer and the Eu complexes only act as the “dopant” [41]. When a forward voltage is applied, the carbazole groups near the interface are oxidized and holes are generated (ON-state). With the increase in forward bias, holes are transported from the polymer/anode interface to the bulk through the neighboring carbazole groups. Since the PKEu chains are saturated, carriers probably do not move along the polymer chain. Instead, they hop between neighboring carbazole groups (either on the same or neighboring polymer chains) [53]. The carbazole group has a tendency to form a partial or full face-to-face conformation with the neighboring carbazole groups. As a result, the region of electron delocalization is extended [54]. When the voltage reaches the threshold voltage of +4 V, the reduced Eu complex can form a CT complex with the surrounding (intra-chain and/or inter-chain) oxidized carbazole species. Because of the presence of a large redox potential difference ($\Delta E_{\text{redox}} = 2.8$ V) in PKEu, the CT complex is basically insulating (to achieve a highly conductive

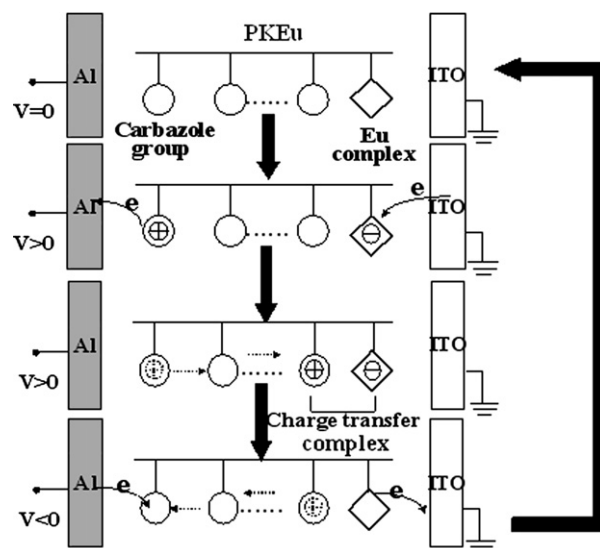


Fig. 7. The oxidation, reduction and charge migration processes in the copolymer PKEu during memory device operation (write/erase) (Ref. [41]).

CT complex, the ΔE_{redox} between the donor and the acceptor must be in the range of -0.25 V to 0.25 V [55]. Now the material is in its low conductivity state (OFF-state). The CT complex so-formed is not very stable because of the steric hindrance of the Eu complex. A reversal of voltage can attract the holes (detrapping) from the bulk back to the interface to recombine with the electrons, resulting in the return of the carbazole groups and Eu complexes to their original states (erase) [41].

In addition to Eu complex, further incorporation of an electron acceptor, 1,3,4-oxadiazole moiety (Ox), can improve the performance of the memory device to result in a shorter response time, longer retention time and higher ON/OFF ratio [42]. The additional electron acceptor can act as a mediator to facilitate carrier transport from the respective HOMOs and LUMOs of the carbazole (Cz) and Eu components. The mediation effect reduces internal energy barriers and accelerates hole transport from the HOMO of Cz and electron transport from the LUMO of Eu when a threshold voltage is applied [42].

4. Bistable electrical switching based on charge transfer processes in polymers

4.1. Materials and structural features

Some polyimides (PIs) containing electron donor and electron acceptor groups (Scheme 2) are capable of exhibiting bistable electrical switching arising from field-induced CT processes. For example, in TPS-PI, the triphenylamine groups act as electron donors, the imide groups act as the electron acceptors. Polyimides are widely used in the microelectronics industry [56], owing to their excellent mechanical strength,

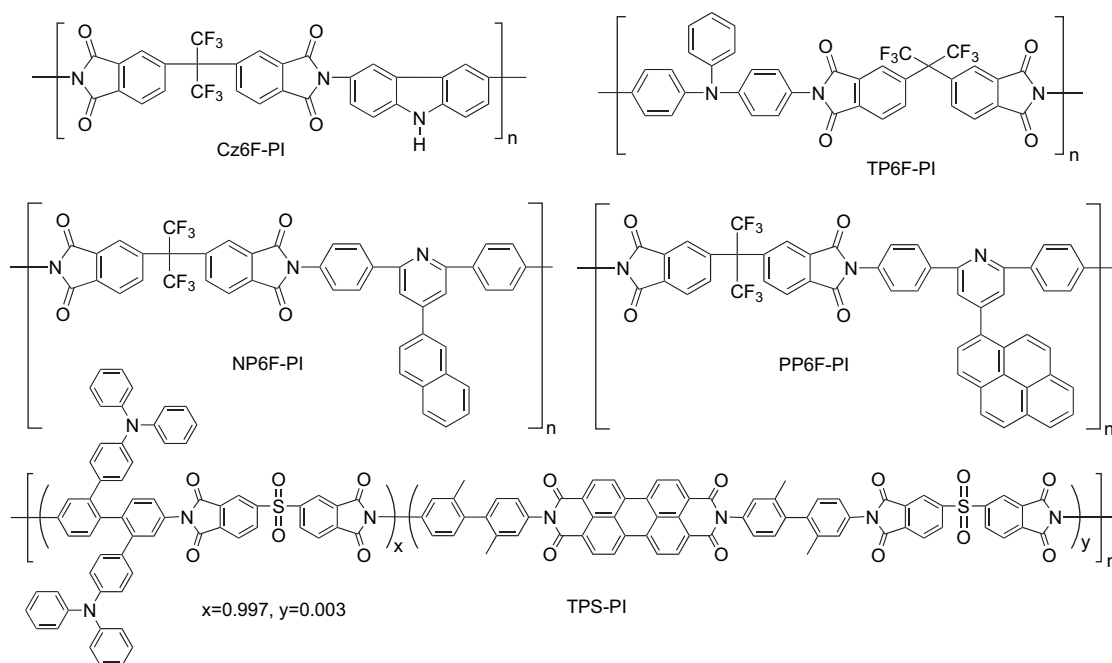
superior thermal and chemical stabilities, and low dielectric constants [57,58]. The Langmuir–Blodgett (LB) technique has been used to fabricate memory devices based on PIs [59], and scanning probe microscopes, such as STM and AFM, have been used as probe electrodes in memory characterization [60]. LB films of PI are usually prepared by thermal imidization (at about 300 °C for 10 min) of the poly(amic acid)-(*N,N*-dimethyl-*n*-hexadecylamine) salt LB films [61]. Physical and molecular packing defects commonly found in LB films may affect the reliability and performance of electronic devices which incorporate these films [62]. As an alternative to the LB technique, PIs with hexafluoroisopropyl groups are soluble in organic solvents and thus can be cast into films directly from solution.

4.2. Memory effects and current–voltage characteristics

It is possible to tune the memory properties by tailoring the molecular structure of PIs. By selecting PIs with electron donating and/or withdrawing groups of proper strengths, and with suitable arrangements of the donors and acceptors in the structure, memory device based on these PIs can behave as a DRAM (using TP6F-PI and Cz6F-PI), a non-volatile and rewritable flash memory (using PP6F-PI and NP6F-PI) and a WORM memory (using TPS-PI).

4.2.1. WORM memory effect from TPS-PI

The memory effect of TPS-PI is illustrated by the J – V characteristics of an ITO/TPS-PI/Al device (Fig. 8). When swept positively from 0 V to 5 V, J is in the order of 10^{-8} – 10^{-5} A/cm², indicating that the device is initially at its low conductivity state (OFF-state, or “0” signal in data storage). In the 1st sweep from 0 V to -7 V, an abrupt increase in J



Scheme 2. Chemical structures of some functional polyimides exhibiting charge transfer-induced memory effects.

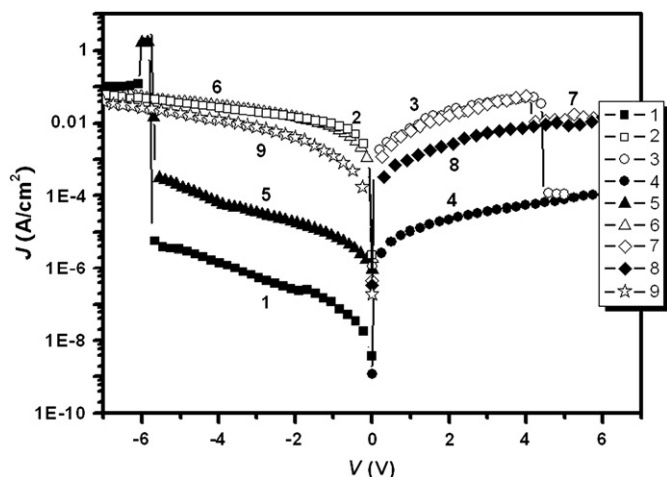


Fig. 8. J - V characteristics of the ITO/TPS-PI/Al device for two sweep directions. The numbers in the figure indicate sweep sequence.

occurs at the switching threshold voltage of about -5.7 V, indicating the device transition from a low conductivity state to a high conductivity state (ON-state, or the “1” signal in data storage). This electrical transition from the OFF-state to the ON-state serves as the “writing” process for the memory device. The distinct bi-electrical states in the voltage range of 0 to -5.7 V allow a voltage (e.g., -1.0 V) to read the “0” signal (before writing) and “1” signal (after writing) of the memory. The device remains in this high conductivity state during the subsequent negative scan (the 2nd sweep in Fig. 8) and even after the power is turned off. When the device is swept positively while in the ON-state (the 3rd sweep), an abrupt decrease in J occurs at the threshold voltage of about $+4.4$ V, corresponding to the “erasing” process for the memory device. The device remains in this low conductivity state during the subsequent positive sweep (the 4th sweep) and even after the power is turned off. It should be noted that the memory device is not completely reset to the initial low conductivity state, since J of the erased state is about 2 orders of magnitude higher than that of the initial OFF-state. However, the erased state can be similarly re-written to the ON-state, when swept negatively (the 5th sweep), and retained in the ON-state (the 6th sweep). The subsequent attempt to erase the ON-state by a positive sweep (the 7th sweep) only results in a small drop in J . In the subsequent negative sweep (the 9th sweep), J increases steadily to the ON-state without an abrupt increase. The results indicate that, although the device has the capability for rewriting, its erasing capability is rather poor. Thus, this device can be used as a WORM-type memory rather than a flash type memory.

4.2.2. Flash memory effect from PP6F-PI

The I - V characteristics of the ITO/PP6F-PI/Al sandwich structure are shown in Fig. 9. The device is at its low conductivity state (OFF-state) initially and I increases progressively with the applied bias (stage I). A sharp increase in injection current occurs between $+4$ V and $+5$ V (stage II), indicating the transition of the device from the OFF-state to the high

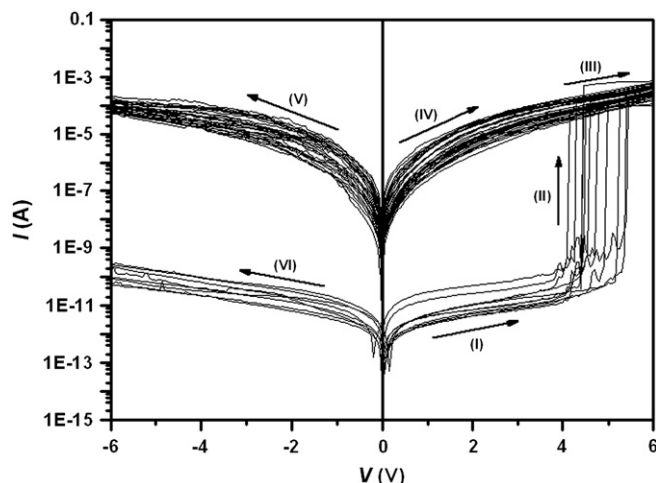


Fig. 9. Current-voltage (I - V) characteristics of a 0.4×0.4 mm² ITO/PP6F-PI/Al device. The magnitude of I , but not the current density, was dependent on the electrode area. The high conductivity (ON) state was “erased” by an applied -5 V voltage pulse of 2-s duration.

conductivity state (ON-state). The transition from the OFF-state to the ON-state is equivalent to the “writing” process in a digital memory cell. After this transition, the device remains in the ON-state when further swept forward to $+6$ V (stage III). After this “writing” process, the device remains in its high conductivity state during the subsequent positive or negative sweeps, as well as after the power has been turned off (stages IV and V). The distinct dual electrical states in the voltage range of 0 V to $+4$ V allow the use of a voltage (e.g., $+2.0$ V) to read the “0” signal (before writing) and “1” signal (after writing) of the memory. The I - V characteristics not only define the electrical bistability of PP6F-PI, but also reveal the non-volatile nature of the memory effect.

One of the most important features of the present polymer memory is that the OFF-state can be recovered by the simple application of a reverse voltage pulse of -5 V for 2 s. This is equivalent to the “erasing” process of a digital memory cell. The device remains in this low conductivity (“0”) state during the subsequent negative sweeps and even after the power is turned off (stage VI). The erased (“0”) state can be further written to the stored (“1”) state when the device is swept positively again to the switching threshold voltage, indicating that the memory device is completely rewritable. As shown in Fig. 9, the I - V characteristics are repeatable with good accuracy and device degradation is not observed. The small variations in transition voltage and current during different sweeps are likely to be due to the inherent relaxation property of the polymer. The ability to write, read, erase and rewrite the electrical states of the device fulfils the functionality of a flash memory.

4.2.3. DRAM effect from TP6F-PI

The ITO/TP6F-PI/Al device exhibits DRAM behavior [63], and its J - V characteristics are shown in Fig. 10. The device is initially at its low conductivity state. When a switching

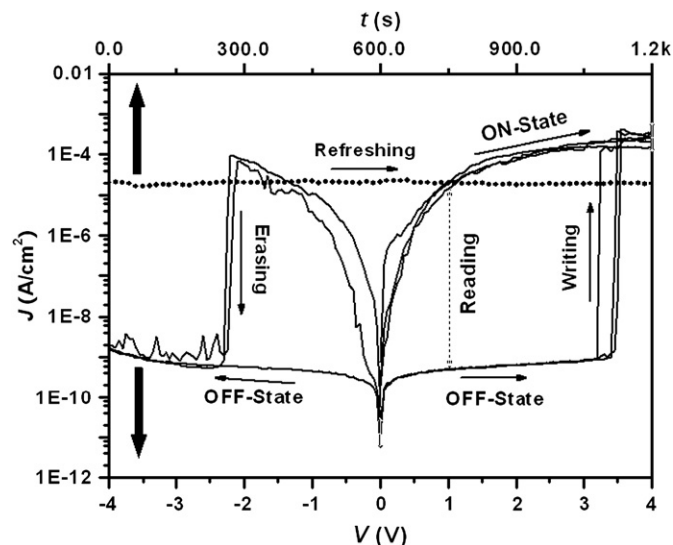


Fig. 10. The J - V characteristics of a 0.16 mm^2 ITO/PP6F-PI/Al device. The writing, reading, erasing and refreshing processes and sweep directions are indicated in the figure (Ref. [63]).

threshold voltage of about $+3.2 \text{ V}$ is applied, an abrupt increase in J can be detected, indicating the device transition from a low conductivity state to a high conductivity state (the “writing” process). The device remains in this high conductivity state during the immediate and subsequent sweeps in the same direction as the switching threshold voltage (Fig. 10). However, when the device is swept in the reverse bias direction, or pulsed at an erasing threshold voltage of about -2.1 V , or when the power is switched off, it returns to the stable OFF-state. The switching behavior indicates that the memory effect is volatile. The erased (“0”) state can be further written to the stored (“1”) state when the switching threshold voltage is re-applied, indicating that the memory device is rewritable. The short retention time of the unstable ON-state indicates that the memory device is volatile. However, the unstable ON-state can also be electrically sustained by a refreshing voltage pulse. This ability to write, read, erase and refresh the electrical states of the device fulfils the functionality of a DRAM [63].

4.3. Operating mechanism and electronic processes

The mechanism of high-field induced conductivity may be similar to the photoinduced electron transfer mechanism commonly observed in many photoconductive PI systems [64]. In the absence of an electric field, the charge transfer excitons have no net dipole moment, because there are as many states polarized to the right as to the left within the PI films, and thus can give rise to the CT photoluminescence. In the presence of an applied field, the right and left polarized states do not have the same energy and there should therefore be a splitting of the original CT exciton states. In view of the distinct dipolar nature of these CT excitons, it is possible to move these excitons by the application of an intense electric field [65]. The presence of a high enough electric field can also quench the CT

photoluminescence to generate the charge carriers [66]. Molecular simulation of a model imide compound, *N*-phenylphthalimide, was carried out using Fujitsu MOPAC 2000 with AM1 as the potential function [67]. Fig. 11 shows the resulting LUMO and HOMOs of *N*-phenylphthalimide. The LUMO is located on the phthalimide group (acceptor), while the first and second HOMOs are located on the phenylamine group (donor). The plausible processes induced by an electric field are shown in Fig. 11. At the threshold voltage, one of the electrons at the third HOMO transits to the LUMO within the phthalimide group and forms the excited state. Excitation of the acceptor leads to an increased electron affinity of the acceptor, and consequently promotes charge transfer at the excited state. Electron transfer can occur from the HOMO of the phenylamine group to the third HOMO of the phthalimide group to form a conductive CT complex (Fig. 11). Due to the presence of the two carbonyl substituents on the nitrogen atom, the electron donating ability of the phenylamine group is much lower than the electron-accepting ability of the phthalimide group. The incorporation of electron donor groups can result in an enhancement of photocurrent by several orders of magnitude, as compared to the donor-free PI [68]. This enhancement has resulted from the improved CT complex formation in the PI backbone [68]. In TP6F-PI, triphenylamine acts as an electron donor, while phthalimide as an electron acceptor to promote the CT complex formation. The charges can be further segregated under an electric field and delocalized to the conjugated triphenylamine, thus stabilizing the CT state to some extent. However, the ON-state of TP6F-PI could not be sustained due to limited charge delocalization in the triphenylamine moieties. A reverse bias of about -2.1 V , or removal of the electric field, can dissociate the CT complex and return the

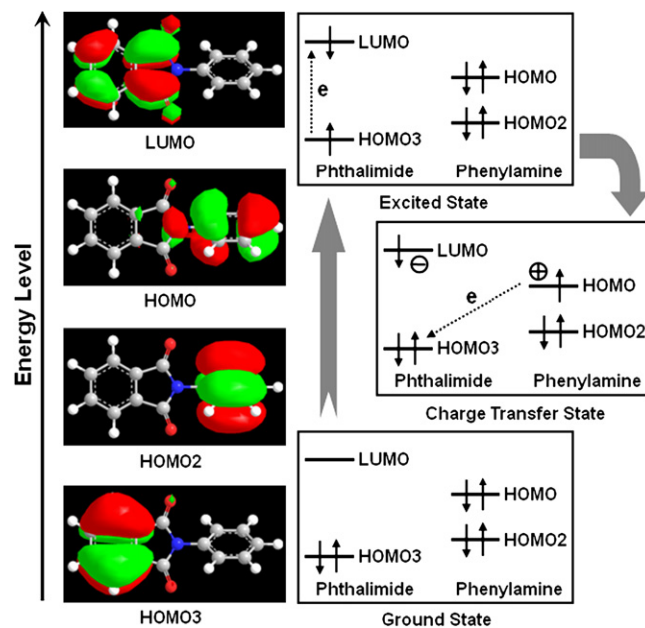


Fig. 11. Molecular orbitals (left) of the model compound, *N*-phenylphthalimide, and electronic processes (right) from the ground state to the charge transfer state induced by the electric field.

device to the initial OFF-state. Thus, the device based on TP6F-PI exhibits DRAM effect.

Differing from the TP6F-PI, the electron donor group of PP6F-PI (the pyrene moiety) is present as a pendant group rather than in the backbone. With this difference in structure, PP6F-PI has a much lower HOMO energy level (-5.40 eV) and a higher dipole moment (2.28 Debye) in comparison to those of TP6F-PI (-4.93 eV and 2.06 D, respectively). The lower HOMO energy level may explain the higher switch-on voltage required for the memory device based on PP6F-PI, while the higher dipole moment leads to a more stable CT structure. Thus, the device based on PP6F-PI exhibits the non-volatile and rewritable flash memory behavior. In TPS-PI, the triphenylamine moieties act as the electron donors, the sulfonyldiphthalimide groups serve as the electron acceptors, and the perylene moieties with the highly delocalized charge carriers provide the conductive channels, to improve the CT complex formation and charge transportation. It is found that the charges can be further segregated under a high electric field and delocalized to the large conjugated moieties nearby, resulting in the formation of a very stable CT complex. Thus, the high conductivity state of TPS-PI can be maintained for a long period even after the removal of the electric field, and it cannot be erased to the initial low conductivity state within the experimentally applied bias. The device based on TPS-PI, therefore, functions as a WORM memory. Thus, it is possible to tune the memory properties by tailoring the molecular structure of PIs.

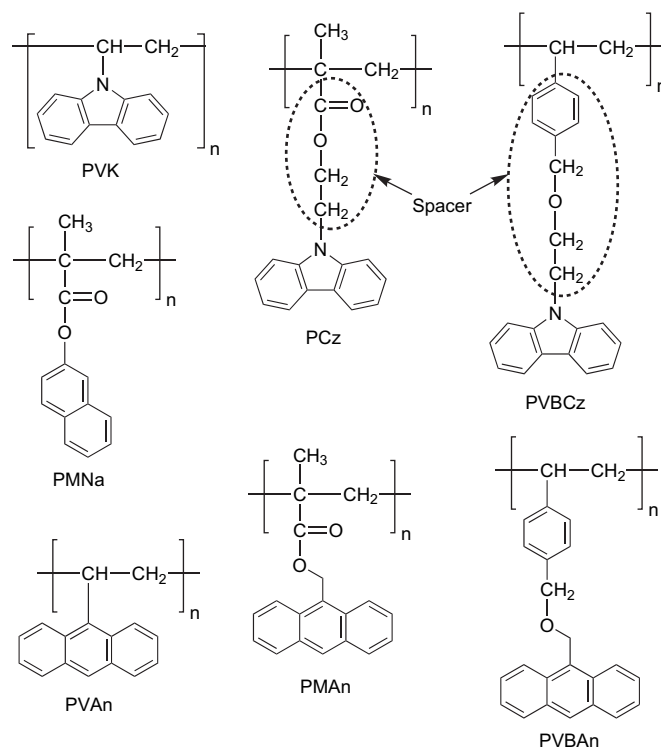
5. Conformation-induced conductance switching in polymers

5.1. Materials and structural features

The memory switching effect was firstly observed in thin (600 nm) tetracene films sandwiched between aluminium and gold electrodes in 1969 [69]. After that, several acene derivatives including naphthalene [70], anthracene [70–72], pentacene [73], and the like, have been reported. In recent years, some acenyl moieties, such as anthracenyl and naphthalenyl, have been incorporated into polymers [74–77]. Polymeric materials have obvious advantages, such as ease of preparation, diversity in backbone structures, and higher thermal stability, compared to small organic molecular acenes. Scheme 3 shows some polymers with or without a flexible spacer ($\text{O}=\text{C}-\text{O}-\text{C}-\text{C}$ and phenyl- $\text{C}-\text{O}-\text{C}-\text{C}$ units) for bridging the electroactive pendant chromophore, such as carbazole (Cz), naphthalene (Na) and anthracene (An). These isolated chromophores can facilitate charge carrier (hole or electron) injection and transport from the electrodes when induced by light irradiation or an electric field. Many of these polymers have been used as photoconductive, xerographic and charge transport materials [56,78–81].

5.2. Memory effects and current–voltage characteristics

Poly(2-(9*H*-carbazol-9-yl)ethyl methacrylate), or PCz, is a non-conjugated polymer containing an electron donating



Scheme 3. Chemical structures of polymers, with or without a flexible spacer unit for the pendant electroactive group, for the conformation-induced memory effects.

carbazole pendant group attached to the main chain by an ethylacrylate unit [82]. Fig. 12(a) shows the J – V characteristics of the ITO/PCz/Al device. The top Al electrode and bottom ITO electrode are connected to a varying voltage source. The bottom ITO is grounded and the current passing through the electrodes is monitored. For the as-fabricated device, the conductivity is very low. The as-fabricated device shows the current density of the low conductivity state ($\sim 10^{-6}$ A/cm², OFF-state) at a read voltage of -1 V. By sweeping the voltage from 0 V to -3 V, a switch in the conductivity state is observed [82]. Upon reaching the threshold voltage of around -1.8 V, the device switches from the low conductivity (OFF) state to a high conductivity (ON) state with a current density of ~ 1 A/cm². The device remains in the ON-state as the voltage is swept from -1.8 V to -3 V. With subsequent sweeping of the voltage under negative bias, the current density is characteristic of that of the ON-state current in Fig. 12(a). The device ITO/PCz/Al thus exhibits WORM memory behavior as it is both non-rewritable and non-volatile after it has been switched ON [82]. The devices based on polymer containing anthracenyl moiety with a similar linker (such as PMAAn) also exhibit non-volatile memory effects, while the devices based on polymers with a longer and bulkier spacer (such as PVBCz) exhibit volatile memory effects. In the absence of a spacer unit between the pendant group and the main chain, PVK does not exhibit memory switching effects. Fig. 12(b) shows the J – V characteristics of an equivalent ITO/PVK/Al device. Using a similar sweep from 0 V to -3 V, the device exhibits only a single ON-state, without any discernible conductance switching [82].

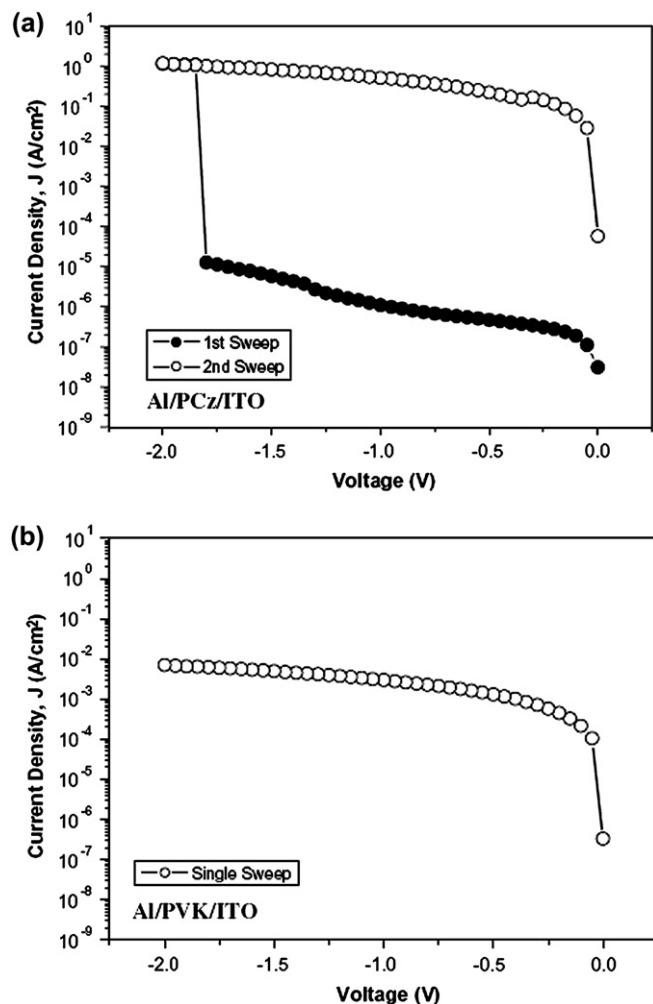


Fig. 12. (a) Typical J - V characteristics of an Al/PCz/ITO device in the ON- and OFF-state, showing an OFF-ON transition when voltage = -1.8 V. (b) Typical J - V characteristics of the Al/PVK/ITO device, showing PVK always exhibiting an ON-state (Ref. [82]).

5.3. Operating mechanism and electronic processes

Compared to that of PVK, the well-defined memory property of PCz can be attributed to the presence of the spacer between the pendant carbazole group and the polymer backbone. In PVK, the neighboring carbazole (Cz) groups have a high tendency to form the face-to-face conformations in the ground state [54]. As a result, the region of electron delocalization is extended to several Cz groups. The charge carriers (holes) can be shared as such and hop through the regioregular Cz groups in the direction of electric field [41]. In PCz, the flexible molecular spacer between the Cz group and the backbone does not favor interaction of the neighboring Cz groups, but promotes them to form regiorandom structure at the ground state [82]. The charge carriers (holes) will have difficulty hopping through the neighboring carbazole groups due to the absence of the face-to-face conformation and the long distance between the neighboring carbazole groups [82]. However, driven by the applied field, the charged carbazole group has the tendency to attract the nearby neutral carbazole groups to form

partial or full face-to-face conformation. The positive charge will then be delocalized to neighboring carbazole groups through the more ordered conformation. As the delocalization process increases with the increase in electric field up to the required threshold value, the carbazole groups in the bulk material transform from a regiorandom to a regioregular structure, in the general direction of the electric field towards the Al cathode [82]. As a result, a high conductivity path among the hole-transporting carbazole groups is established and the device is switched to its ON-state. The oxidized carbazole groups are further stabilized by the neighboring electron-withdrawing $-O-C=O$ groups [82]. After the device is switched to the ON-state, it cannot be reverted back to the initial regiorandom structure, even by applying a reverse bias of higher magnitude than the switching voltage. Once the conduction pathways are formed under an applied field, they facilitate charge transport under both biases and the device cannot be switched off by applying a reverse voltage. Thus, the device based on PCz behaves as a WORM electronic memory [82].

For the volatile memory effect involving PVBCz, the phenyl group in the spacer is a less efficient transporter of charges than the carbazole group, thus hindering the formation of continuous transport pathways. The more amorphous nature of PVBCz also means that the carbazole groups are further apart in the ground state and the charge transport pathways formed by conformational changes may be shorter (more difficult to influence the adjacent carbazole group) or less continuous. Thus, the change in conductivity due to conformational changes is limited. As a result, the ON-state current density and the ON/OFF current ratio of PVBCz device are lower than those in the corresponding PCz devices. Similar to that of the PCz device, once the conduction pathways are formed under an applied electric field, they facilitate charge transport under both biases. Thus, the PVBCz device also cannot be switched off by applying an opposite bias or a higher voltage of the same bias. However, the PVBCz device can return to the OFF-state through conformational relaxation since there is sufficient conformational freedom provided by the benzyloxyethyl spacer unit.

Fig. 13(a) and (b) shows, respectively, the optimized geometries of PVK and PCz at the ground state. PVK exists in the face-to-face conformation, while PCz is in a regiorandom conformation. The structure difference between PVK and PCz is also revealed by the X-ray diffraction (XRD) and field-emission transmission electron microscopy (FE-TEM) results. The XRD spectra in Fig. 13(c) reveal an additional diffraction peak at $2\theta = 8^\circ$ for PVK, which is attributable to the crystalline microdomains of PVK. The nearest face-to-face distance is about 11.384 Å. The XRD spectrum for PCz shows only a broad amorphous peak at 2θ of about 20° [82]. Fig. 13(d) and (e) shows the FE-TEM images of PVK and PCz before voltage sweeps. The PVK film shows crystalline microdomains, while the PCz film is amorphous and homogeneous. However, as shown in the high resolution TEM images of Fig. 13(f) and (g), crystalline microdomains have also appeared in the PCz film after the device has been transformed to the high conductivity ON-state (using the TEM Cu grid as the bottom electrode and a removable Hg droplet as the top electrode). Thus, the field-induced

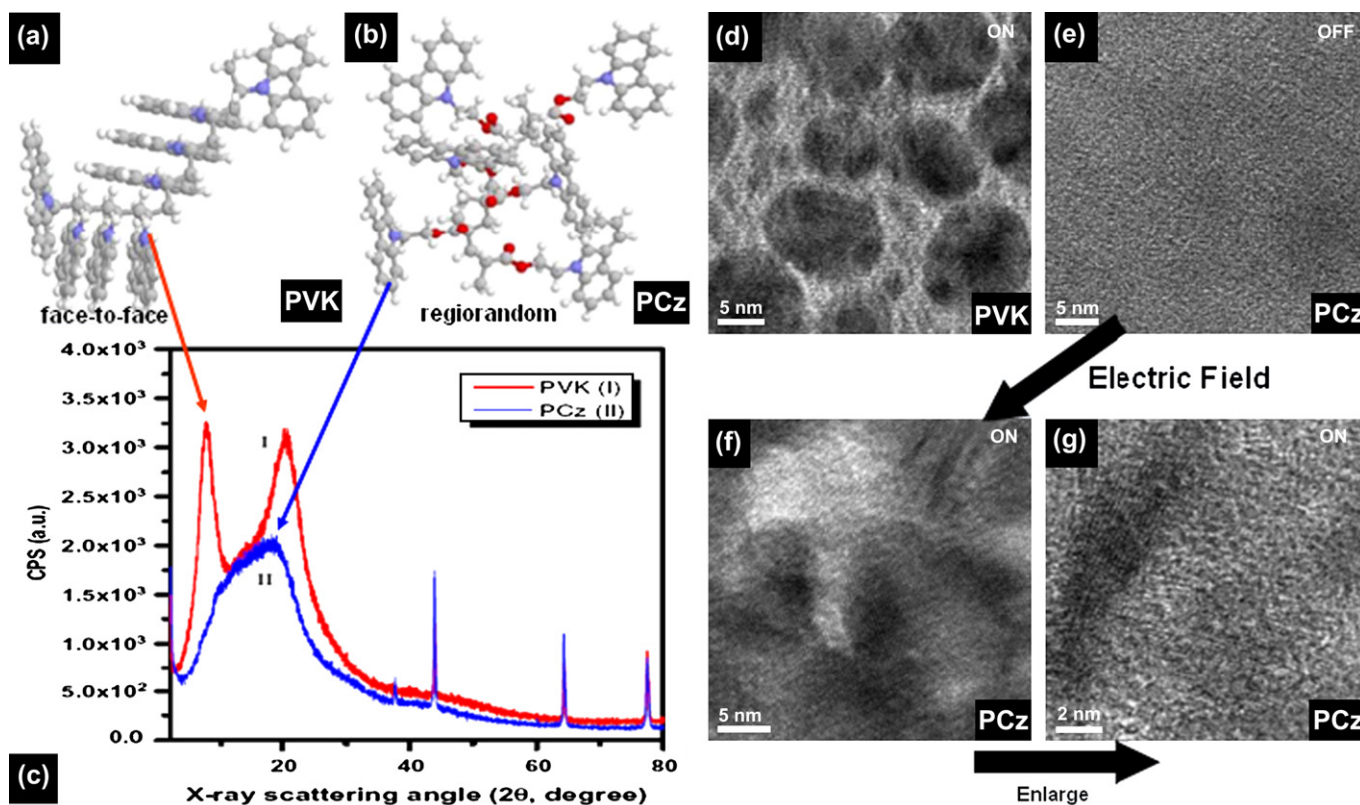


Fig. 13. (a) and (b) Simulation results by molecular mechanics showing the optimized geometry corresponding to the minimized energy states in PVK and PCz. (c) X-ray diffraction patterns of PVK and PCz at ground state (Ref. [82]). (d)–(g) FE-TEM images of PVK and PCz before and after transformation to high conductivity state under electric field.

conformational ordering (OFF- to ON-state switching) and retention of the ordered state (ON-state) in these non-conjugated polymers with electroactive pendant chromophore groups have been ascertained [82].

6. Bistable conductance switching based on redox effects in polymer nanocomposites

6.1. Materials and structural features

Nanomaterials, such as fullerene [83,84], carbon nanotube [85] and gold nanoparticles [38,86,87], are also used as nanotraps. Most of them are doped into polymer matrices to form composite materials and to facilitate solution processing during device fabrication. Flash and WORM memories have been realized in some nanocomposite materials. Fig. 14(a) shows the composite material of PVK and gold nanoparticles (AuNP), which serve as the electron donors and acceptors, respectively. As shown in the FE-TEM image and the size distribution charts of Fig. 14(c) and (d), respectively, the size of the gold nanoparticles is in the range of 1.5–6.5 nm [88]. As an effort to design and synthesize polymers with the necessary electronic properties for the single component memory device, PVK modified by covalently tethered fullerene (PVK-C₆₀, Fig. 14(b)), which contains about 4 wt% C₆₀ or *x*:*y* ~ 0.99:0.01, has been synthesized. In PVK-C₆₀, the carbazole groups act as the electron donors and the C₆₀ serves as the electron acceptor [89]. Thus, for

the PVK:AuNP nanocomposite, the nanomaterial (AuNP) is physically doped into the PVK matrix, while for the PVK-C₆₀ compound, the nanomaterial (fullerene) is chemically bonded to the PVK backbone.

6.2. Memory effects and current–voltage characteristics

Both the devices based on PVK:AuNP and PVK-C₆₀ exhibit non-volatile, rewritable flash memory effects. The memory effect of the device Al/PVK:AuNP/TaN is suggested by the *J*–*V* curves shown in Fig. 15(a) [88]. The *J*–*V* curves are recorded by scanning from 0 V to 4 V and then going back to 0 V. The device distinctively displays two conductivity states. With an applied voltage on the as-fabricated device, the current increases slowly with the voltage and remains low. The current density is in the range of 10^{–8} A/cm² at 1 V. This is the low conductivity state (OFF-state). When the applied voltage is increased further to ~3 V, a sharp increase in the current is observed, indicating the device transition from the OFF-state to a high conductivity state (ON-state) [88]. For the programmed device, it shows a high current for the voltage applied and the current density at 1 V is about 10^{–3} A/cm². This current density is 5 orders of magnitude higher than that in the OFF-state. The distinct bi-electrical states in the voltage ranging from 0 V to 2 V allow a low voltage (e.g., 1.0 V) to read the “0” or “OFF” signal (before writing) and “1” or “ON” signal (after writing) of the device [88]. Curve

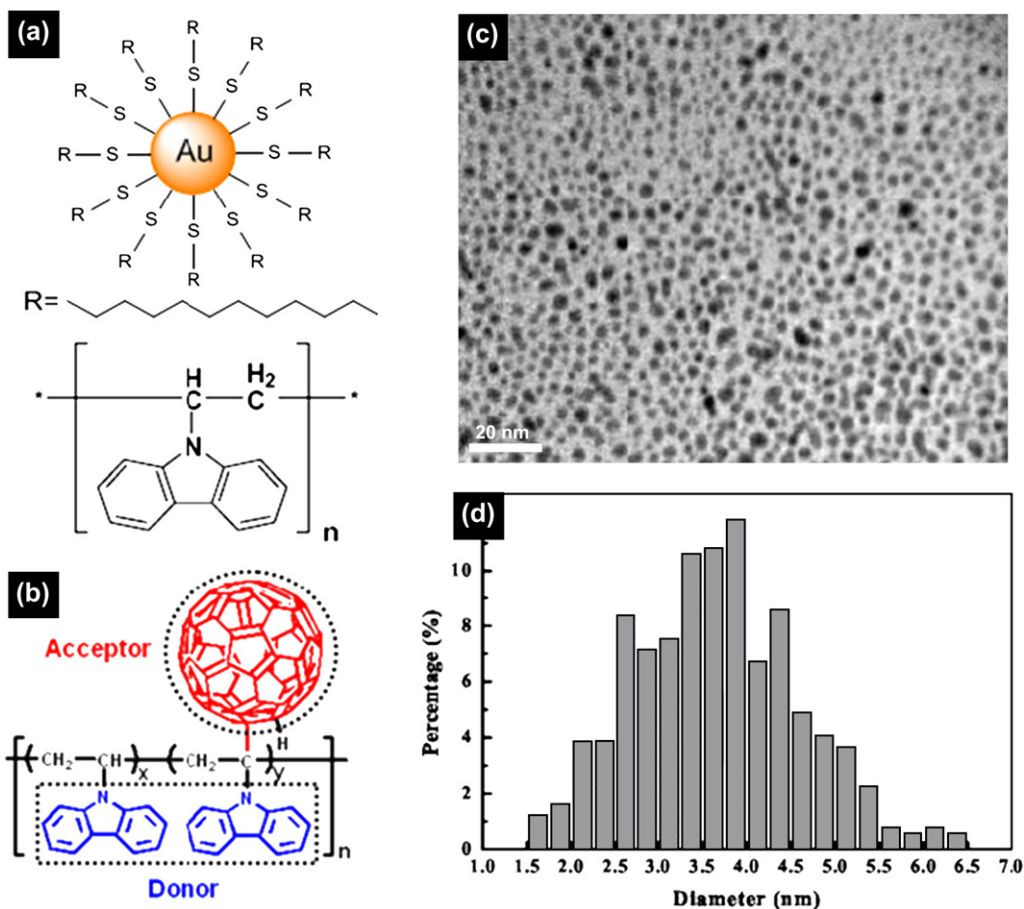


Fig. 14. (a) and (b) Structures of PVK:AuNP composite material and the copolymer of *N*-vinylcarbazole and fullerene (PVK:C₆₀, wherein *x*:*y* ~ 0.99:0.01) (Ref. [89]). (c) and (d) Size of gold nanoparticles (determined by FE-TEM) and their distribution (Ref. [88]).

2 in Fig. 15(a) shows a sweep from 0 V to 4 V after the first sweep. It can be seen that the device, after reaching its high conductivity state, remains in this ON-state even after turning off the power. The ON-state can be erased to the OFF-state by applying a reverse bias, as indicated by curve 3, where the current density suddenly drops to 10⁻⁸ A/cm² at -1.7 V. The erased state (“0”) could be further written to the high

conductivity state (“1”) when the switching threshold voltage is re-applied (curve 4), indicating that the memory device is rewritable and non-volatile [88].

The *J*–*V* characteristics of an ITO/PVK–C₆₀/Al sandwich device are shown in Fig. 15(b) [89]. Initially, the device is swept positively (with ITO as the cathode, Al as the anode) from 0 V to 4 V. The device remains in the low conductivity state without

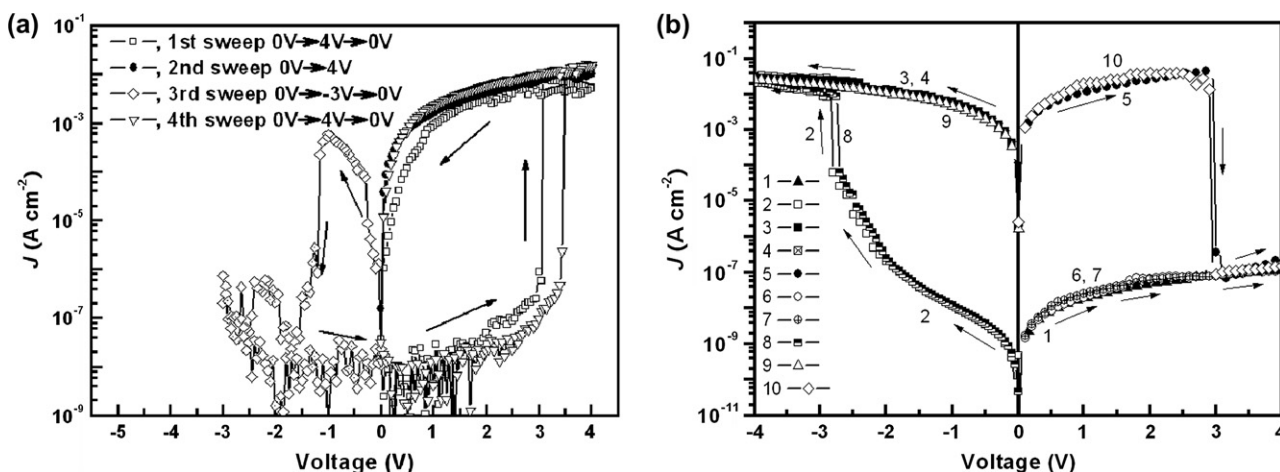


Fig. 15. The *J*–*V* characteristics of the (a) Al/PVK:AuNP/TaN and (b) ITO/PVK–C₆₀/Al devices (Refs. [88,89]).

any abrupt increase in current density. However, when it is swept negatively (with ITO as the anode, Al as the cathode) from 0 V to -4 V, J increases progressively with the applied bias and a sharp increase in injection current occurred at about -2.8 V (the 2nd sweep), indicating the device transition from a low conductivity state (OFF-state) to a high conductivity state (ON-state) [89]. The device exhibits good stability in this high conductivity state during the subsequent negative sweep (the 3rd sweep). It remains in the ON-state even after turning off the power (the 4th sweep). The J – V characteristics define the electrical bistability of PVK– C_{60} and also reveal the non-volatile nature of the memory effect. The ON-state can be recovered by the simple application of a reverse voltage of about 3.0 V (the 5th sweep). The 6th and 7th sweeps show the J – V characteristics of the device right after the application of an erase sweep and turning off the power, respectively [89]. The J – V characteristics are nearly identical to those of the 1st sweep, indicating that the device remains in the stable OFF-state. This feature allows the application of PVK– C_{60} in a rewritable memory device. The above J – V characteristics of the device are repeatable with high accuracy. Sweeps 8, 9

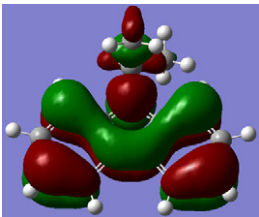
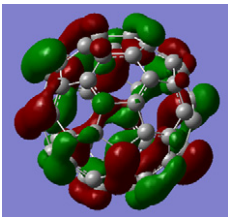
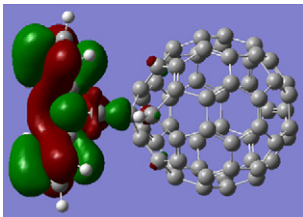
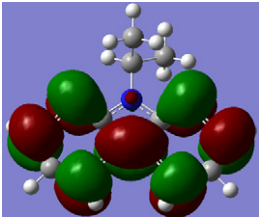
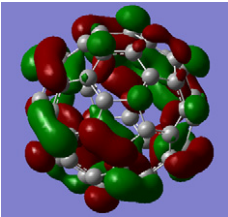
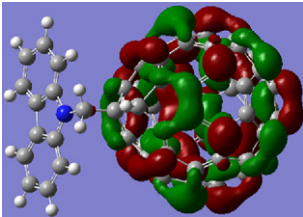
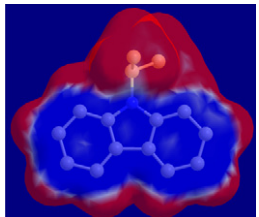
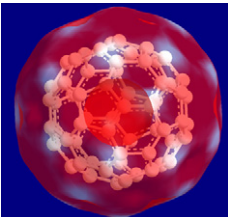
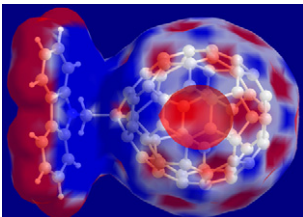
and 10 are the J – V characteristics of the device after 20 write–read (ON)–erase–read (OFF) switching cycles. With the decrease in active area ($0.16 \rightarrow 0.04 \rightarrow 0.0225 \text{ mm}^2$) of the device, the current magnitude decreases accordingly. However, the current density remains almost constant, indicating the absence of sample degradation or dielectric break-down [89].

6.3. Operating mechanism and electronic processes

Electrical bistability and memory effects in the Al/PVK: AuNP/TaN and ITO/PVK– C_{60} /Al devices are due to charge transfer from the electron donor PVK to the electron acceptor nanomaterials. The operating mechanism and electronic processes are elucidated with the latter as the representative device.

Table 2 shows the simulation results for fragments and basic unit of PVK– C_{60} by DFT B3LYP 6-31G(d) method [89]. Vinylcarbazole (VK) has a lower HOMO energy level (value) than that of C_{60} , indicating that the VK group has a stronger tendency to donate an electron. The electron-withdrawing

Table 2
Molecular simulation results for the components in PVK– C_{60} (Ref. [89])

Components	VK	C_{60}	VK- C_{60}
HOMO (energy level)	 (-5.116 eV)	 (-6.014 eV)	 (-5.469 eV)
LUMO (energy level)	 (-0.435 eV)	 (-3.129 eV)	 (-2.748 eV)
Bandgap	4.681 eV	2.885 eV	2.721 eV
Dipole Moment ^a	1.93 Debye	0.00 Debye	3.32 Debye
ESP ^b			
Total Energy	-635.4 Hartree ^c	-2286.2 Hartree	-2842.6 Hartree

^a Field-independent basis dipole moment.

^b Molecular electrostatic potential surface (mapped with total charge density).

^c 1 Hartree = 4.36×10^{-18} J.

ability of C_{60} is indicated by a high LUMO energy level. It has been reported that a C_{60} molecule can become negatively charged and can capture up to six electrons [90]. When these two components are covalently connected, the HOMO of PVK- C_{60} is located on the carbazole side, while the LUMO of PVK- C_{60} is located on the C_{60} side. This feature promises easier charge transfer from carbazole (HOMO) to C_{60} (LUMO). The dipole moment data show that C_{60} is a non-polar and symmetric molecule, while carbazole is slightly polar with a total dipole moment of 1.93 Debye. When these two components are covalently connected, the total dipole moment is 3.32 Debye, which is almost comparable to that of a highly polar molecule, such as HCl (3.57 Debye). This phenomenon indicates that there is a high tendency for charge separation in PVK- C_{60} , as well as a good ability for PVK- C_{60} to retain charges once induced by an electric field [89].

The HOMO and LUMO energy levels of PVK- C_{60} , together with the work function of electrodes, are shown in Fig. 16(a) [89]. When ITO is used as the anode and Al as the cathode (negative sweep), the energy barriers of ITO/HOMO and Al/LUMO interfaces are only around 0.7 eV. For the reverse case, the energy barriers of Al/HOMO and ITO/LUMO are 1.2 eV. The relatively high energy barriers prevent switching of the device to the ON-state during the positive sweep. Charge injections are more favorable during the negative sweep [89]. The high HOMO energy level of the

carbazole moiety indicates that PVK- C_{60} is a p-type material with the holes as the dominant charge carriers since carbazole is the dominant moiety in PVK- C_{60} . However, under a low bias, hole mobility in PVK- C_{60} is blocked by the C_{60} moieties with a low HOMO energy level. The device is at the low conductivity state (OFF-state) [89]. When the electric field exceeds the energy barrier (~ 0.7 eV), holes are injected into the HOMO of the carbazole moieties and electrons are injected into the LUMO of C_{60} . The charged HOMO of the carbazole moiety and the charged LUMO of C_{60} form a channel for charge carriers through charge transfer interactions, as illustrated in Fig. 16(b). The polymer becomes p-doped under the induction of the electric field and switches to the high conductivity state (ON-state). Due to the strong electron-withdrawing ability of C_{60} , its high LUMO energy level, and the strong dipole moment between PVK and C_{60} , electrons trapped in C_{60} can be retained and coexist with the surrounding positively charged carbazole moiety (Fig. 16(b)). As a result of the dipole formation, an internal electric field is created, maintaining the high conductivity state. Under a reversed bias of about +3 V, C_{60} loses the charged state to neutralize the positively charged carbazole moiety. The internal electric field disappears immediately and the device returns to its initial low conductivity state (OFF-state).

7. Performances of polymer memories

Some parameters, including write/erase/read voltages, ON/OFF current ratio, write–read–erase–read (WRER) cycle, switching time, retention ability, and stability under voltage stress or read pulses, are of importance to the performance of a polymer memory device. Evaluation results for some of these parameters are shown in Fig. 17. These parameters were evaluated under ambient conditions.

Fig. 17(a) shows the ON/OFF current ratio as a function of applied voltage for the same sweep for the device Al/PF6Eu/ITO. An ON/OFF current ratio as high as 10^7 has been achieved. The high ON/OFF current ratio promises a low misreading rate through the precise control over the ON- and OFF-state [44]. Fig. 17(b) shows the effect of continuous read pulses on the ON- and OFF-state of the device Al/PF6Eu/ITO. The inset shows the pulses used for the measurements. No resistance degradation is observed for the ON- and OFF-state after more than 10^8 read cycles, indicating that both states are insensitive to read cycles [44]. Fig. 17(c) shows the stability of the device ITO/PVK- C_{60} /Al under a constant stress voltage for 12 h [89]. Although a slight change in the ON- and OFF-state current density is observed, an ON/OFF current ratio of 10^6 can be maintained and the stability can be further projected to 10 years, indicative of the stability of both the material and the electrode/polymer interfaces [89]. Fig. 17(d) shows the transient response of current versus time of the device Al/PKEu/ITO. The inset shows the circuit layout used in the measurement. The memory device has a switching time of about 20 μ s from the ON-state to the OFF-state [41]. The switching time is almost comparable to that (~ 1 μ s) of a NAND (NOT/AND) flash memory based

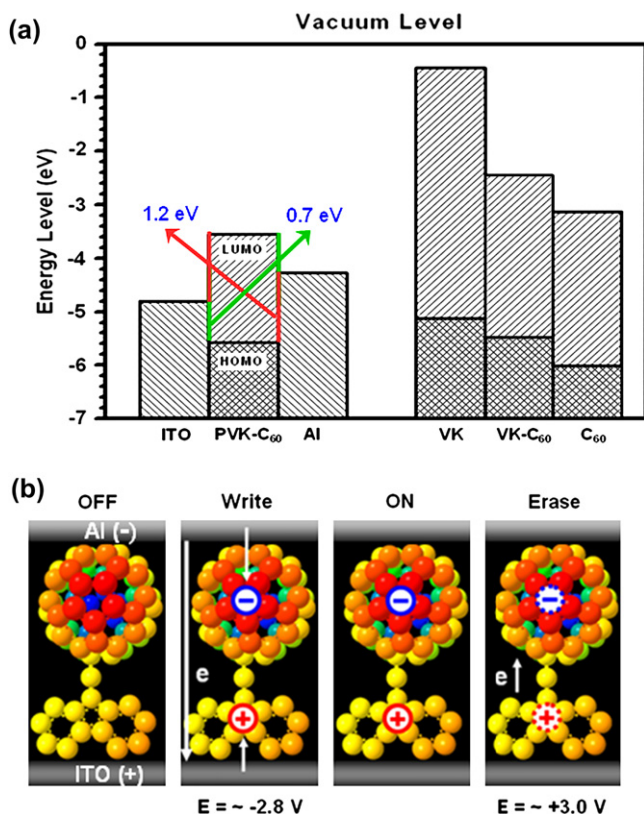


Fig. 16. (a) The energy band diagram of PVK- C_{60} (from CyV results) and its molecular components (from calculation results). (b) Plausible electronic processes in a molecule of VK- C_{60} producing the memory effects (Ref. [89]).

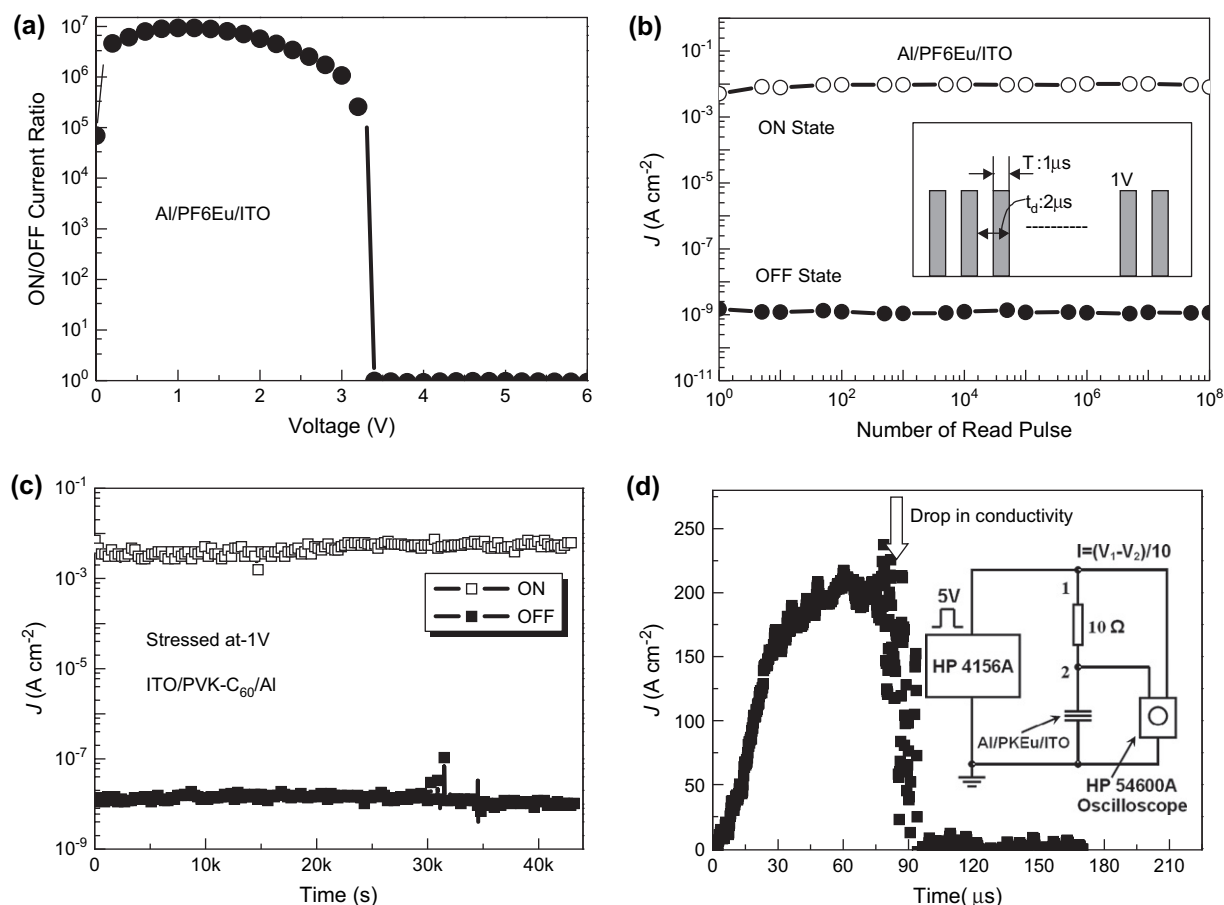


Fig. 17. Some performance results for polymer memories. (a) ON- to OFF-state current ratio as a function of applied voltage for the same sweep (Ref. [44]). (b) Effect of 1 V read pulses on the device current density in the OFF-state and ON-state. The inset shows the pulses used for the measurements (Ref. [44]). (c) Effect of operation time (at -1 V) on the device current density in the OFF-state and ON-state tested under ambient conditions. The inset shows the ON- to OFF-state current ratio as a function of applied voltage for the same sweep (Ref. [89]). (d) Transient response of current versus time, showing the switching time from ON- to OFF-state. The inset shows the corresponding circuit used in the measurement (Ref. [41]).

on the traditional semiconductors. Memory devices based on polymeric ferroelectric materials, with a switching time of the order of 50 μs , have been suggested for use in data storage [91]. Thus, the device based on PKEu is a relatively fast access

memory. The response time is probably fast enough for data storage in many hand-held device applications [91]. The performance parameters of the other polymer memories are summarized in Table 3.

Table 3
Summary of the performance evaluation results of the polymer memories

Devices	Memory effects	Write voltage (V)	Erase voltage (V)	Read voltage (V)	Refresh voltage	ON/OFF ratio	Read pulses	Switching time	Stress time (h)	Reference
Al/PKEu/ITO	Flash	-2.0	+4.0	-1.0	—	10^4	10^6	20 μs	3	[41]
ITO/PCzOxEu/Al	Flash	-2.8	+4.4	+1.0	—	10^5	10^6	1.5 μs	8	[42]
Al/PF6Eu/ITO	WORM	+3.0	—	+1.0	—	10^7	10^8		3	[44]
Al/PF6Eu/n-Si	WORM	+2.2	—	+1.0	—	10^4	10^8		12	[47]
Al/PF8Eu/ITO	WORM	+3.0	—	+1.0	—	10^6	10^7	$\sim 1 \mu\text{s}$	10	[45,46]
PPy/P6FBEu/Au	WORM	+4.0	—	+1.0	—	200	10^6		3	[48]
ITO/PFOxPy/Al	DRAM	-2.8	+3.5	-1.0	-1 V/10 s	10^6	10^8		12	[51]
ITO/PCz/Al	WORM	-1.8	—	-1.0	—	10^6	10^7	1 ms	12	[82]
ITO/PVK-C ₆₀ /Al	Flash	-2.8	+3.0	+1.0	—	10^5	10^8		12	[89]
ITO/TPS-PI/Al	WORM	-5.7	—	-1.0	—	10^5	10^8		12	
ITO/PP6F-PI/Al	Flash	~ 4.5	-5.0	+2.0	—	10^6	10^8		7	
ITO/TP6F-PI/Al	DRAM	+3.2	-2.1	+1.0	1 V/5 s	10^5	10^8		5	[63]
Al/PVK: AuNP/TaN	Flash	+3.0	-1.7	+1.0	—	10^5		1.0 μs	12	[88]

8. Summary

The demand for smaller, lighter and more compact devices, that can perform more complicated functions, work faster, and juggle more data, are pushing conventional semiconductor technology to its limits. Plastic electronics are potential alternatives. A number of polymeric electronic devices, including transistors, switches, wires, lasers, sensors, photovoltaic cells and light-emitting diodes, have already been realized. Polymeric memories will play an increasingly important role in plastic electronics.

Researchers at the National University of Singapore and the Institute of Microelectronics in Singapore have successfully produced several data storage devices based on designed polymers, having the required electronic properties within a single macromolecule. These devices exhibit distinctive bistable conductivity (OFF- and ON-) states, which are accessible by applying a switching threshold voltage. The electrical bistability can be induced by trapping–detrapping, charge transfer, conformational change, or nanocomposite redox effects. This feature (electrical bistability) allows the fabrication of polymer memories based on the high (encodes “1” signal) and low conductivity (encodes “0” signal) responses to an applied voltage. The molecular structure of polymers can be tailored, through functionalization with electron donors and acceptors of different strengths, with spacer moieties of different steric effects for the electroactive pendant groups, or by incorporating nanostructured electroactive materials, to induce different memory behaviors in simple metal/polymer/metal devices. Several polymer memory effects, including rewritable flash memory, write-once read-many-times (WORM) memory and dynamic random access memory (DRAM) have been realized. These polymer memory devices exhibit a high ON/OFF current ratio, promise low misreading rates, and can endure more than one million read cycles. Both the ON-state and OFF-state are stable under constant voltage stress. These polymer memories also have a relatively fast response time in the microsecond range, making them suitable for many data storage applications.

References

- [1] Waser R. *Nanoelectronics and information technology: advanced electronic materials and novel devices*. 2nd ed. Weinheim: Wiley-VCH; 2005.
- [2] Service RF. *Science* 2003;302(5645):556–7.
- [3] Compano R. *Nanotechnology* 2001;12(2):85–8.
- [4] Raymo FM. *Adv Mater* 2002;14(6):401–14.
- [5] Chen SH, Shiau CS, Tsai LR, Chen Y. *Polymer* 2006;47(26):8436–43.
- [6] Reed MA, Zhou C, Muller CJ, Burgin TP, Tour JM. *Science* 1997;278(5336):252–4.
- [7] Bandyopadhyay A, Pal AJ. *Adv Mater* 2003;15(22):1949–52.
- [8] Kushida M, Inomata H, Miyata H, Harada K, Saito K, Sugita K. *Jpn J Appl Phys* 2003;42(6A):622–4.
- [9] Liu CY, Pan HL, Fox MA, Bard AJ. *Chem Mater* 1997;9(6):1422–9.
- [10] Mukherjee B, Pal AJ. *Appl Phys Lett* 2004;85(11):2116–8.
- [11] Potember RS, Poehler TO, Cowan DO. *Appl Phys Lett* 1979;34(6):405–7.
- [12] Hoagland JJ, Wang XD, Hipps KW. *Chem Mater* 1993;5(1):54–60.
- [13] Muller R, Genoe J, Heremans P. *Appl Phys Lett* 2006;88(24):242105-1-3.
- [14] Iwasa Y, Koda T, Tokura Y, Koshihara S, Iwasawa N, Saito G. *Appl Phys Lett* 1989;55(20):2111–3.
- [15] Xue ZQ, Gao HJ, Liu WM, Wu QD, Chen HY, Qiang D, et al. *Jpn J Appl Phys* 1994;34(1):197–9.
- [16] Tour JM. *Adv Mater* 1994;6(3):190–8.
- [17] Tour JM. *Chem Rev* 1996;96(1):537–53.
- [18] James DK, Tour JM. *Aldrichimica Acta* 2006;39(2):47–56.
- [19] Roth KM, Dontha N, Dabke RB, Gryko DT, Clausen C, Lindsey JS, et al. *J Vac Sci Technol B* 2000;18(5):2359–64.
- [20] Liu ZM, Yasseri AA, Lindsey JS, Bocian DF. *Science* 2003;302(5650):1543–5.
- [21] Liu ZM, Schmidt I, Thamyongkit P, Loewe RS, Syomin D, Diers JR, et al. *Chem Mater* 2005;17(14):3728–42.
- [22] Kevorkian J, Labes MM, Larson DC, Wu DC. *Discuss Faraday Soc* 1971;51:139–43.
- [23] Swiatek J. *Thin Solid Films* 1977;41(1):5–8.
- [24] Ma LP, Yang WJ, Xue ZQ, Pang SJ. *Appl Phys Lett* 1998;73(6):850–2.
- [25] Shi DX, Ba DC, Pang SJ, Gao HJ. *Appl Surf Sci* 2001;182(1–2):64–8.
- [26] Ling QD, Zhu CX, Chan DSH, Kang ET, Neoh KG. *Molecular and polymer memories*. In: Nalwa HS, editor. *Encyclopedia of nanoscience and nanotechnology*. 2nd ed. American Scientific Publishers; 2007.
- [27] Yang Y, Ouyang J, Ma LP, Tseng RJ, Chu CW. *Adv Funct Mater* 2006;16(8):1001–14.
- [28] Fu L, Cao LC, Liu YQ, Zhu DB. *Adv Colloid Interface Sci* 2004;111(3):133–57.
- [29] Li C, Fan WD, Lei B, Zhang DH, Han S, Tang T, et al. *Appl Phys Lett* 2004;84(11):1949–51.
- [30] Guizzo E. *IEEE Spectrum* 2004;41(4):17–8.
- [31] Yang Y, Ma LP, Wu JH. *MRS Bull* 2004;29(11):833–7.
- [32] Service RF. *Science* 2001;293(5536):1746.
- [33] Scott JC. *Science* 2004;304(5667):62–3.
- [34] Stikeman A. *Technol Rev* 2002;105(7):31.
- [35] Dennler G, Lungenschmied C, Neugebauer H, Sariciftci NS, Latreche M, Czeremuszkin G, et al. *Thin Solid Films* 2006;511:349–53.
- [36] Yakisir D, Mighri F, Bousmina M. *Macromol Rapid Commun* 2006;27(18):1596–602.
- [37] Moller S, Perlov C, Jackson W, Taussig C, Forrest SR. *Nature* 2003;426(6963):166–9.
- [38] Ouyang J, Chu CW, Szmanda CR, Ma LP, Yang Y. *Nat Mater* 2004;3(12):918–22.
- [39] Chu CW, Ouyang J, Tseng HH, Yang Y. *Adv Mater* 2005;17(11):1440–3.
- [40] Zhong G, Kim K, Jin JI. *Synth Met* 2002;129(2):193–8.
- [41] Ling QD, Song Y, Ding SJ, Zhu CX, Chan DSH, Kwong DL, et al. *Adv Mater* 2005;17(4):455–9.
- [42] Ling QD, Wang W, Song Y, Zhu CX, Chan DSH, Kang ET, et al. *J Phys Chem B* 2006;110(47):23995–4001.
- [43] Fang JF, You H, Chen JS, Lin J, Ma DG. *Inorg Chem* 2006;45(9):3701–4.
- [44] Ling QD, Song Y, Teo EYH, Lim SL, Zhu CX, Chan DSH, et al. *Electrochem Solid-State Lett* 2006;9(8):268–71.
- [45] Song Y, Ling QD, Zhu C, Kang ET, Chan DSH, Wang YH, et al. *IEEE Electron Device Lett* 2006;27(3):154–6.
- [46] Song Y, Tan YP, Teo EYH, Zhu CX, Chan DSH, Ling QD, et al. *J Appl Phys* 2006;100(8):84508.
- [47] Tan YP, Ling QD, Teo EYH, Song Y, Lim SL, Lo PG, et al. 2006 MRS Spring Meeting, San Francisco, CA, United States. Warrendale, PA 15086, United States: Materials Research Society; 2006. p. 114–19.
- [48] Li L, Ling QD, Lim SL, Tan YP, Zhu C, Chan DSH, et al. *Org Electron* 2007;8(4):401–6.
- [49] Bez R. *Microelectron Eng* 2005;80:249–55.
- [50] Hua ZY, Chen GR. *Vacuum* 1992;43(11):1019–23.
- [51] Ling QD, Song Y, Lim SL, Teo EYH, Tan YP, Zhu CX, et al. *Angew Chem Int Ed* 2006;45(18):2947–51.

- [52] Birnbaum ER, Forsberg JH, Marcus Y, Sc Y. In: Moeller T, editor. La–Lu rare earth elements. Gmelin handbook of inorganic chemistry. 8th ed., vol. 39. New York: Springer-Verlag; 1981. p. 65–232.
- [53] Safoula G, Napo K, Bernede JC, Touihri S, Alimi K. Eur Polym J 2001;37:843.
- [54] Vandendriessche J, Palmans P, Toppet S, Boens N, De SF, Masuhara H. J Am Chem Soc 1984;106(26):8057–64.
- [55] Zhu DB, Zhang B, Qin W. Organic conductor and superconductor. In: Zhu DB, Wang FS, editors. Organic solid. Shanghai, PR China: Shanghai Science and Technology Press; 1999. p. 48–88.
- [56] Claudius F, Hilmar F. Polyimides in high-performance electronics packaging and optoelectronic applications. In: Ghosh MK, Mittal KL, editors. Polyimides: fundamentals and applications. New York: Marcel Dekker; 1996. p. 759–814.
- [57] Meador MA. Annu Rev Mater Sci 1998;28:599–630.
- [58] Yudin VE, Otaigbe JU, Gladchenko S, Olson BG, Nazarenko S, Korytkova EN, et al. Polymer 2007;48(5):1306–15.
- [59] Takimoto K, Kawade H, Kishi E, Yano K, Sakai K, Hatanaka K, et al. Appl Phys Lett 1992;61(25):3032–4.
- [60] Yano K, Kyogaku M, Kuroda R, Shimada Y, Shido S, Matsuda H, et al. Appl Phys Lett 1996;68(2):188–90.
- [61] Sakai K, Kawada H, Takamatsu O, Matsuda H, Eguchi K, Nakagiri T. Thin Solid Films 1989;179(1–2):137–42.
- [62] Leisieur P, Barraud A, Vandevyver M. Thin Solid Films 1987;152(1–2):155–64.
- [63] Ling QD, Chang FC, Song Y, Zhu CX, Liaw DJ, Chan DSH, et al. J Am Chem Soc 2006;128(27):8732–3.
- [64] Tokita Y, Ino Y, Okamoto A, Hasegawa M, Shindo Y, Sugimura N. Jpn J Polym Sci Technol 1994;51(4):245–50.
- [65] Pope M, Swenberg CE. Electronic processes in organic crystals and polymers. 2nd ed. New York: Oxford University Press; 1999.
- [66] Pearson JM. Pure Appl Chem 1977;49(4):463–77.
- [67] Basu R, Chowdhury M. J Indian Chem Soc 2005;82(10):909.
- [68] Freilich SC. Macromolecules 1987;20:973–8.
- [69] Szymanski A, Larson DC, Labes MM. Appl Phys Lett 1969;14(3):88–90.
- [70] Garrett SG, Pethig R, Soni V. J Chem Soc Faraday Trans 2 1974;70:1732–40.
- [71] Vityuk NV, Fedchuk AP, Mikho VV. Sov Phys Solid State 1975;17(3):612–3.
- [72] Elsharkawi AR, Kao KC. J Phys Chem Solids 1977;38(1):95–6.
- [73] Tondelier D, Lmimouni K, Vuillaume D, Fery C, Haas G. Appl Phys Lett 2004;85(23):5763–5.
- [74] Arias AC, Huemmelgen IA, Meneguzzi A, Ferreira CA. Adv Mater 1997;9(12):972–4.
- [75] Ma DG, Aguiar M, Freire JA, Hummelgen IA. Adv Mater 2000;12(14):1063–6.
- [76] Mello RM, Azevedo EC, Meneguzzi A, Aguiar M, Akcelrud L, Hummelgen IA. Macromol Mater Eng 2002;287(7):466–9.
- [77] Jiang YM, Wan XG, Guo F, Xie HB, Liu P, Li J. Phys Status Solidi A 2005;202(9):1804–7.
- [78] Grazulevicius JV, Strohriegel P, Pielichowski J, Pielichowski K. Prog Polym Sci 2003;28(9):1297–353.
- [79] Hasegawa M, Horie K. Prog Polym Sci 2001;26(2):259–335.
- [80] Pearson JM, Stolka M. Poly (*N*-vinylcarbazole). New York: Gordon and Breach Scientific Publishers, Inc.; 1981.
- [81] Qu JQ, Kawasaki R, Shiotsuki M, Sanda F, Masuda T. Polymer 2006;47(19):6551–9.
- [82] Teo EYH, Ling QD, Song Y, Tan YP, Wang W, Kang ET, et al. Org Electron 2006;7(3):173–80.
- [83] Paul S, Kanwal A, Chhowalla M. Nanotechnology 2006;17(1):145–51.
- [84] Majumdar HS, Baral JK, Osterbacka R, Ikkala O, Stubb H. Org Electron 2005;6(4):188–92.
- [85] Pradhan B, Batabyal SK, Pal AJ. J Phys Chem B 2006;110(16):8274–7.
- [86] Tseng RJ, Ouyang J, Chu CW, Huang JS, Yang Y. Appl Phys Lett 2006;88(12):123506.
- [87] Paul S, Pearson C, Molloy A, Cousins MA, Green M, Koliopoulou S, et al. Nano Lett 2003;3(4):533–6.
- [88] Song Y, Ling QD, Lim SL, Teo EYH, Tan YP, Li L, et al. IEEE Electron Device Lett 2007;28(2):107–10.
- [89] Ling QD, Lim SL, Song Y, Zhu CX, Chan DSH, Kang ET, et al. Langmuir 2007;23(1):312–9.
- [90] Dresselhaus MS, Dresselhaus G, Eklund PC. Science of fullerenes and carbon nanotubes. San Diego: Academic Press; 1996.
- [91] Weiss R. Electron Des 2001;49(17):56–64.



En-Tang Kang received his B.A. degree in chemistry from the University of Nebraska at Lincoln in 1976, his B.S. degree in chemical engineering from the University of Wisconsin-Madison in 1978, and his Ph.D. degree in chemical engineering from the State University of New York at Buffalo in 1983. He joined the Department of Chemical and Biomolecular Engineering at the National University of Singapore in 1984 and is currently a professor of the department. His research interest is in exploring new roles of polymers in nanoscience, molecular electronics and biomolecular engineering. He is a Co-Editor of the Journal of Adhesion Science and Technology.



Qi-Dan Ling is a research staff of the Department of Chemical and Biomolecular Engineering at the National University of Singapore. He studied chemistry and polymer science at Fujian Normal University, China, where he received his B.Sc. and M.Sc. degrees in 1993 and 1996, respectively. He received his Ph.D. degree in 2000 from Zhejiang University, China. His research areas include organic synthesis, polymer memory, polymer light-emitting diodes and molecular simulation.



Der-Jang Liaw received his B.S. degree in chemistry from Cheng Kung University (Taiwan) in 1970, his M.S. degree in Polymer Science from Osaka University (Japan) in 1975 and his Ph.D. degree in polymer science from the Osaka University (Japan) in the group of Professors Nozakura and Kamachi. He was an Associate Professor in 1978–1982 and a Professor from 1982 to present in National Taiwan University of Science and Technology. He is on the Editorial Advisory Board of Polymer Journal (Japan), Editorial Board of Polymer International (UK), Editorial Board of Journal of Polymer Research (1994–2001) and Advisory Board of High Performance Polymers (UK). His

research interests are in synthesis and characterization of functional polymer material and high performance polymer via precision polymerization.



Eric Yeow-Hwee Teo received the B.Eng. and M.Eng. degrees in Electrical Engineering from National University of Singapore, in 2000 and 2002, respectively. From 2002 to 2005, he worked as a process engineer in Chartered Semiconductor Manufacturing. Currently, he is a research fellow at the Electrical Engineering Department in National University of Singapore and is also working towards the Ph.D. degree in the polymer memory research field.



Daniel Siu-Hung Chan studied Electrical Engineering at the University of Manchester Institute of Science and Technology where he obtained his B.Sc. and M.Sc. degrees, and at Salford University, United Kingdom where he obtained his Ph.D. He joined the Electrical and Computer Engineering Department at the National University of Singapore in 1980 where he is now a Professor. His present research interests are in integrated circuit failure analysis techniques and reliability, and in device physics and technology.



Chunxiang Zhu received the B.Eng. and M.Eng. degrees in electrical engineering from Xidian University, Xi'an, China, in 1992 and 1995, respectively, and the Ph.D. degree in electrical engineering from The Hong Kong University of Science and Technology, Kowloon, Hong Kong, in 2001. He then joined the Department of Electrical and Computer Engineering, National University of Singapore, Singapore, as an Assistant Professor in February 2001. His areas of research interests include high- κ gate-stack technology on Si, Ge, and SiGe substrates for CMOS applications, high- κ dielectrics for MIM capacitors in RF and mixed signal IC application, polysilicon thin-film transistors, and organic/polymeric electronics. He has authored or coauthored over 100 publications in refereed journals and conferences in these areas.

tors, and organic/polymeric electronics. He has authored or coauthored over 100 publications in refereed journals and conferences in these areas.



Koon-Gee Neoh received her degrees (SB and ScD) in chemical engineering from MIT. She is currently a Professor in the Department of Chemical and Biomolecular Engineering at the National University of Singapore. Her research interests include electroactive and photoactive polymers, molecular design and engineering of biomaterials, and nanostructured metal–polymer systems. She serves on the editorial/advisory board of a number of journals including *Langmuir* and *Journal of Environmental Science and Health – Part A*.